



Granite emplacement in orogenic compressional conditions: the La Alberca–Béjar granitic area (Spanish Central System, Variscan Iberian Belt)

Mariano Yenes*, Fernando Álvarez, Gabriel Gutiérrez-Alonso

Departamento de Geología, Universidad de Salamanca, 37008 Salamanca, Spain

Received 5 December 1997; accepted 10 March 1999

Abstract

The La Alberca–Béjar granitic area comprises a set of intrusions of Upper Carboniferous to Lower Permian age located in the hinterland of the Variscan belt of western Spain. Gravity data, anisotropy of magnetic susceptibility, and microstructural studies carried out in the granitoid and its country rocks indicate that the granitoids of this region have tabular and inverted drop shapes and show sub-horizontal magmatic fabrics and SW–NE lineations. The granitoid bodies were intruded episodically, with single intrusive pulses recorded by deformation in the country rocks. All intrusive events took place during D_3 compressive stage, in the core of large D_1 anticlines, and are not related to structures in the country rock. A syn-orogenic emplacement model for granite intrusion in such conditions is proposed. The proposed model implies the activity of coeval emplacement mechanisms and room generation. © 1999 Elsevier Science Ltd. All rights reserved.

1. Introduction

The ascent and emplacement of large granitic bodies in the upper crust takes place in a variety of orogenic contexts. Most cases studied recently have been in extensional situations (Vigneresse, 1983; Hutton, 1988; Bouillin et al., 1993) where the so called ‘space problem’ (Bowen, 1948) can be easily solved by dilation within large tectonic structures that determine the intrusion level and provide enough ‘room’ for the accumulation of magma.

Less commonly reported in the literature are cases where granitoid bodies are emplaced under contractional geodynamic settings, as described by Hutton (1997). In these cases the intrusions are generally related to large tectonic structures such as transpressive shear zones (Brun and Pons, 1981; Hollister and Crawford, 1986; Schmidt et al., 1990; Tobisch and Paterson, 1990; McCaffrey, 1992; Karlstrom et al.,

1993; Ingram and Hutton, 1994), or thrusts (Morand, 1992; D’Lemos et al., 1992; Tribe et al., 1996). Nevertheless, only a few cases report granitoid bodies that have been related to some large scale structure in compressional situations and these have in turn been related to the local extension that takes place in fold hinges, leading to saddle reef type plutons (McCaffrey, 1992; Aller and Bastida, 1996; Collins and Sawyer, 1996).

Magma emplacement under compressive conditions must occur where local tensional stresses occur, such as pull-apart structures or mode I fractures normal to fold axes, which would facilitate the initiation of magma emplacement. Once the emplacement of magma bodies starts, tensional stresses might be amplified by the magma buoyancy.

This paper describes a detailed study of the La Alberca–Béjar granitoid complex in the Spanish Central System of the Iberian Variscan Belt that was previously interpreted to have formed from several, post-orogenic, magmatic pulses (López Plaza and Martínez Catalán, 1987). In contrast with this interpretation, we propose a syn-orogenic emplacement

* Corresponding author.

E-mail address: myo@gugu.usal.es (M. Yenes)

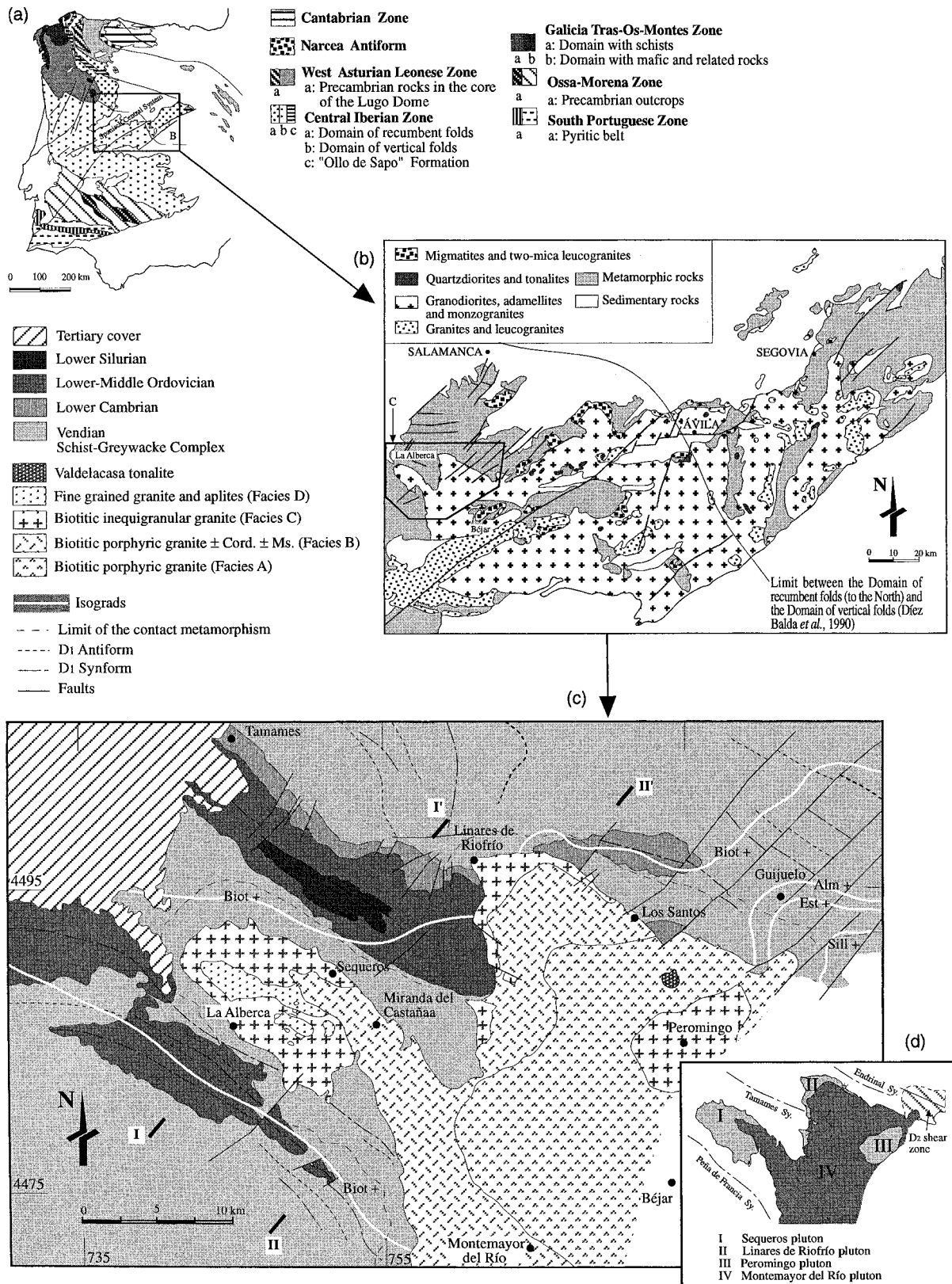


Fig. 1. (a) The Iberian Massif (Julivert et al., 1972) and location of the Spanish Central System. (b) Study area in the northwest termination of the Spanish Central System (map from Fúster and Villaseca, 1987). (c) Geological sketch of the studied area with the location of the cross-sections shown in Fig. 9 and the regional metamorphic zones. (d) The inset depicts the main tectonic structures identified in the country rock and the different plutonic bodies: I—Sequeros; II—Linares de Riofrío; III—Peromingo; IV—Montemayor del Río.

model related to one of the compressional events widely recognized in this sector of the Iberian Variscan Belt. This alternative model for the ascent and emplacement of the Alberca–Béjar granitoid complex arose from the study of three essential aspects of its structural geology: (1) the three-dimensional geometry of the granitoid bodies; (2) their internal structure and (3) the intrusion related deformation of the country rock.

The geometry of the plutonic bodies was established by a combination of three-dimensional gravity data inversion modeling and detailed mapping that has allowed the construction of realistic cross-sections. An AMS survey provided magmatic foliation and lineation data which characterise the internal structure of the plutons. Mapping of the country rock and contact metamorphic aureole, with special attention paid to the microstructural relationships between growth of contact metamorphism minerals and the genesis of regional and local cleavages, has allowed determination of the relative timing of intrusion with respect to the main regional deformation events.

2. Geological setting

The Late Devonian to Early Permian Spanish Central System Igneous Complex (SCSIC) is the most extensive continuous outcrop of granitoids in the Iberian Variscan Belt. The area studied is the north-western end of this complex and it is located in the most internal zone of the orogen, the Central Iberian Zone (CIZ; Fig. 1). The SCSIC lies within a domain characterized by vertical folds according to the division proposed by Díez Balda et al. (1990).

The country rock is composed of a thick sequence of Upper Vendian (Vidal et al., 1994) siliciclastic shales with frequent interbedded sandstones and conglomerates of the Schist–Greywacke Complex, overlain conformably by Lower Cambrian Tamames Sandstones, Tamames Limestone and Endrinal Shales Formations. Ordovician rocks consisting of conglomerates, sandstones and shales culminating with the Armorican Quartzite sequence, crop out in the cores of Variscan synclines. These are overlain by Lower Silurian shales, quartzites and volcanic rocks (Fig. 1).

The structure in the area is known to be related to the Variscan Orogeny where several zones and domains can be distinguished (Fig. 1). In the recumbent fold domain (Fig. 1), the Variscan Orogeny resulted in several phases of NE–SW shortening represented by large NE-verging folds accompanied by ductile, sub-horizontal thrusts involving basement rocks (Macaya et al., 1991). In the vertical fold domain (Fig. 1) the structure can be explained by three superimposed Variscan deformation phases:

- D_1 —Consists of kilometer-scale folds with wavelengths of 10–25 km, horizontal axes and vertical axial planes that develop an axial plane cleavage (S_1). Finite strain analysis (Díez Balda et al., 1994) indicates that D_1 shortening was NE–SW with a horizontal maximum stretching direction, parallel to fold axes. It imparted a planar fabric to the shales ($k = 0.32–0.35$) and a planar–linear fabric to some conglomerates ($k = 0.8–1.7$; k is the Flinn (1962) parameter).
- D_2 —Is related to the extensional collapse of the previously thickened crust during D_1 (Díez Balda et al., 1994). This phase develops narrow shear zones that were originally horizontal with hanging wall movement to the southeast. These shear zones crop out in the area around Guijuelo (Fig. 1), where a horizontal crenulation cleavage occurs (S_2). In the hanging wall, normal faults and NE–SW-trending vertical extension fractures are developed, the latter parallel to the inferred maximum principal paleo-stress direction. The age of this deformation phase is 332 ± 13 Ma (U–Pb in zircons, Galibert, 1984).
- D_3 —This is a compressive episode coaxial with D_1 but less pervasive, leading to large wavelength open folds with vertical axial planes and horizontal axes. The folds develop a local axial plane cleavage (S_3). The Guijuelo–Guijo de Ávila Antiform (Fig. 1) is the best example of a D_3 fold, in whose core, incidentally, the D_2 shear zone outcrops.

Three episodes of regional metamorphism have been identified (Díez Balda et al., 1994): M_1 is an intermediate pressure Barrovian sequence contemporaneous with D_1 crustal thickening, leading to prograde chlorite, biotite, almandine garnet, staurolite and sillimanite zone assemblages; M_2 is related to D_2 extension, is a low pressure metamorphic event characterized by growth of andalusite and cordierite; finally, M_3 is a retrograde event transforming biotite to white mica and chlorite indicating conditions close to the low to medium grade transition during D_3 compression. The isograd distribution of the M_2 event delineates the D_2 shear zone outcrop of the Salamanca Detachment (Díez Balda et al., 1994), the upper limit of the shear zone is located below the upper unit of the garnet zone (Fig. 1).

3. Characteristics of the igneous rocks

The La Alberca–Béjar igneous rocks are quartz monzonites that define an aluminous-calcic series whose genesis is controversial. Some workers claim that they are due to mesocrustal anatexis processes (Bea and Moreno-Ventas, 1985; Franco and García de Figuerola, 1986; Bea and Pereira, 1990), while others

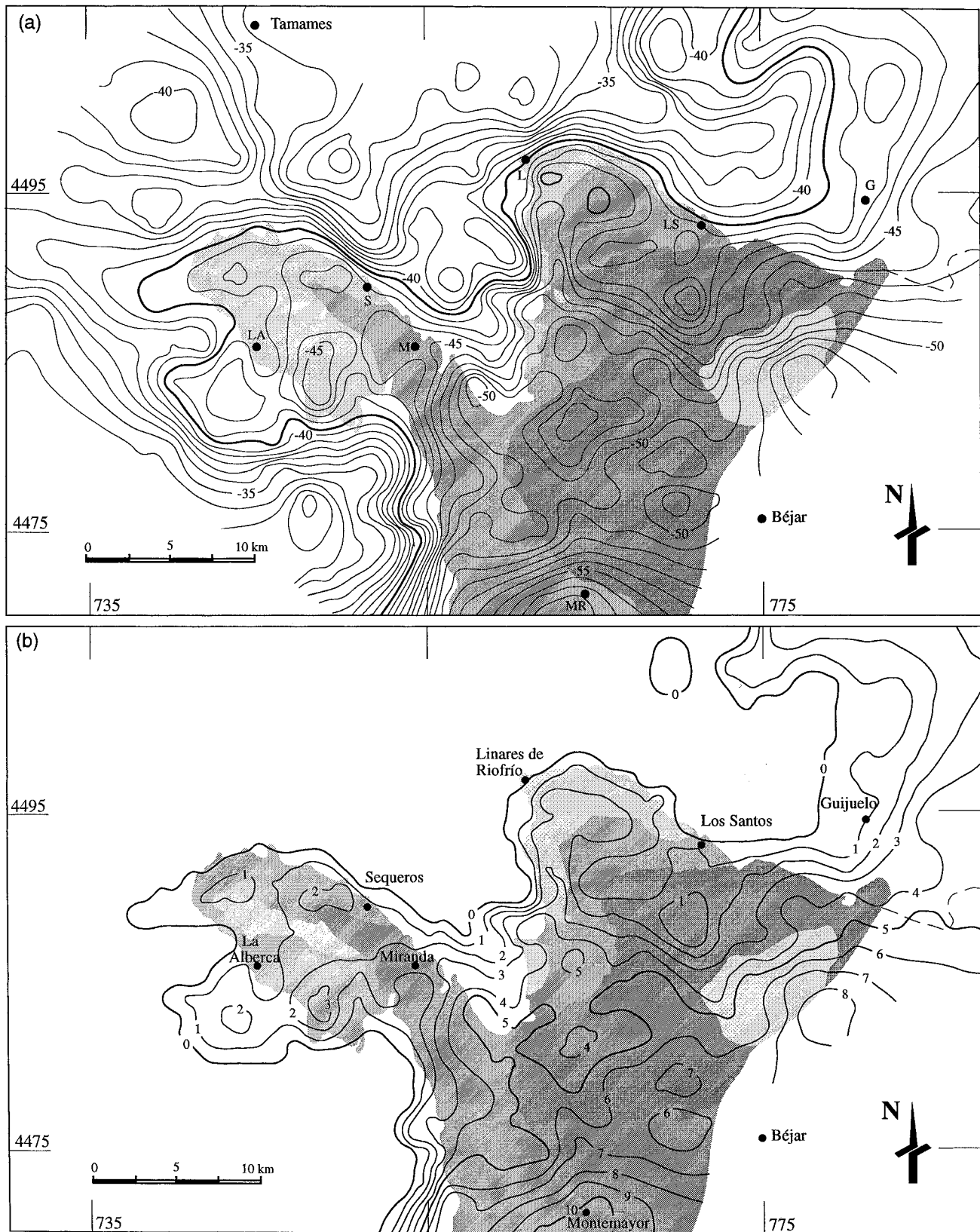


Fig. 2. (a) Bouguer anomaly isovalues map (mGal). The -41 mGal isovalue curve is highlighted (see text for explanation). (b) Map of the modeled thickness (km) of the granitic bodies obtained by means of gravity data inversion. The thickest areas are located south of the plutons, with some deep areas south of the present erosion level of the Sequeros pluton.

invoke a deeper (mantle) origin with metasediment assimilation (Ugidos, 1973; Recio, 1990; Ugidos and Recio, 1993; Moreno-Ventas et al., 1995).

Four main granitic facies (A = Biotitic porphyric granite; B = Biotitic porphyric granite \pm cordierite \pm muscovite; C = Biotitic inequigranular granite and D = Fine grained granite and aplites) have been identified according to the relative abundance and size of alkaline feldspar crystals as well as the occurrence of cordierite (Ugidos et al., 1990) (Fig. 1). The contacts between the two porphyric facies (A and B) are gradual while the contacts of facies C are sharper. The presence of enclaves of facies C in facies A and B indicates the intrusive character of the latter. The contact of facies D is always sharp with the surrounding granitoid rocks. Despite the latter relationships, no deformation has been observed at the contacts between facies, indicating that the different magmatic pulses and intrusions took place consecutively, but not too separated in time; that is, before the complete crystallization of the magma (Yenes, 1996).

The spatial distribution of the different facies, and their intrusive relations, define four plutons (Fig. 1): the Sequeros pluton, the Linares de Riofrío pluton, the Peromingo pluton and the Montemayor del Río pluton.

The separation of these plutons and their intrusive relationships are supported by K/Ar biotite analysis which yielded ages of 281 ± 6 Ma and 280 ± 6 Ma for the Sequeros pluton and 269 ± 6 Ma and 270 ± 6 Ma for the Montemayor del Río pluton (Yenes et al., 1996).

4. Gravity survey

A gravity survey was carried out to constrain the three-dimensional shape of the plutonic bodies (Yenes et al., 1995; Yenes, 1996). Three hundred and eighty-six survey stations were measured using a LaCoste & Ramberg G gravimeter with a total precision of ± 0.01 mGal. The Bouguer anomaly map (Fig. 2a) shows a good correlation between the granite boundary and the -41 mGal curve, except for some local areas (Guijuelo, east of Miranda del Castañar, and south of La Alberca) where the -41 mGal curve extends beyond the granite boundary, revealing the presence of granitic rocks below the country rock that outcrops in that region. Generally there is an increase of the anomaly towards the southeast, that is to say towards the central parts of the SCSIC which can be correlated to the increasing amount of granitoid bodies towards that direction. On the other hand the gravity isovalues in the country rock trends NW–SE, accordingly with the main D_1 structures (La Peña de Francia, Tamames and El Endrinal synclines).

The studied anomaly has been obtained subtracting a flat regional anomaly (-41 mGal) to the local Bouguer anomaly. The subtracted regional anomaly is in agreement with the recommendations made by Vigneresse (1990) leading to a 0 mGal isovalue close to the granitoid contact. We used a three-dimensional data inversion technique (Vigneresse, 1978), based on the iterative method of Cordell and Henderson (1968), to model the shape of the pluton at depth (Fig. 2b). Density values for each pluton and the country rock were obtained through 82 representative samples of all the rocks. As can be appreciated in Figs. 2(a) and (b), the Sequeros and Linares de Riofrío plutons produce an amplitude of the Bouguer anomaly of 8–10 mGal, which indicates an average thickness of the pluton of about 2 km. South of La Alberca, below the Ordovician rocks of the La Peña de Francia syncline, there is an area that shows no outcrop and larger amounts of granite (up to 3 km). South of the Linares de Riofrío pluton a less marked increase in depth is also observed. On the other hand, in the north of the El Endrinal syncline, the modeling suggests a granitic body at depth, that may be up to 2 km deep. Those anomalies could also be caused by sub-outcropping granitoid bodies of Variscan or even pre-Variscan age.

The gravity response of the Montemayor del Río pluton is more marked, with anomalies up to -55 mGal in the southern part, and an average amplitude of the anomaly of about 20 mGal. The Montemayor del Río data indicates model thicknesses of granite from 3 to more than 10 km in the southern part of the region, which contrasts with the thicknesses of the other plutons.

5. Igneous rock structures

5.1. Solid and intermediate state deformations

Microstructural studies of the granitoid samples reveal that all the recognized microstructures that developed under solid and intermediate (Guineberteau et al., 1987; Paterson et al., 1989; Bouchez et al., 1992) state have a uniform geographic distribution, that is to say, there are no particular zones where solid and intermediate state microstructures develop more intensely or with greater abundance, as it could be expected in the contacts of the different plutons. We suggest that this is due to the uniform stress acting during, and subsequent to the final stages of granite emplacement (Benn et al., 1993).

The biotites in the granitoid bodies have developed micro-kinks, which occur both in solid and intermediate state deformations (Tribe and D'Lemos, 1996). In some samples, fractures parallel to the (001) planes are filled with residual fluids of quartz–feldspar compo-

sition, indicating that some deformation occurred during the last stages of magma crystallization; that is, in the intermediate state (Bouchez et al., 1992).

Feldspar crystals develop occasional myrmekitic textures, which are probably related to high temperature, solid-state deformation (Simpson, 1985; Hibbard, 1987; Simpson and Wintsch, 1989; Pryer, 1993). To a lesser extent, some microfractures, such as the ones observed in the biotites, have been recognized implying some degree of intermediate state deformation.

Quartz is the mineral that best records plastic deformation in granitoids under any pressure, temperature, or fluid conditions (e.g. Vauchez, 1980; Marre, 1982; Paterson et al., 1989). In this study, quartz crystals commonly show undulose extinction, but seldom display mosaic structures. This suggests crystallographic control of the orientation of the grain boundaries and their high mobility, which in turn suggests high-temperature deformation processes (Lister and Dornsiepen, 1982; Gapais and Barbarin, 1986). In some cases, basal subgrain boundaries originating by slip of m prismatic crystallographic planes in the $[c]$ axes direction, have been observed. These subgrain boundary systems are activated by high temperature deformation under sub-solidus conditions (Blumenfeld et al., 1986; Gapais and Barbarin, 1986; Mainprice et al., 1986; Bouchez et al., 1987; Aranguren and Tubía, 1992; Tribe and D'Lemos, 1996). In addition to the aforementioned subgrain boundaries, prismatic subgrain boundaries resulting from slip in the $\langle a \rangle$ direction are observed, which suggests lower temperatures and higher strain rates (Hobbs, 1981; Takeshita and Wenk, 1988; Mainprice and Nicolas, 1989).

5.2. Magnetic fabric study

Since J.W. Graham (1954) first demonstrated the anisotropy of magnetic susceptibility (AMS) technique, it has become established as a rapid and precise method to establish the shape fabric exhibited by ferromagnetic and paramagnetic minerals in rocks. Specifically, it has been proven to be useful in granitoid rocks, where the traditional methods of establishing a fabric are difficult to apply. AMS allows the systematic study of the fabric, providing directional data (foliation and lineation) and quantitative parameters related to the rock composition and deformation state.

The magnetic susceptibility (K) is a second order tensor that can be represented geometrically by an ellipsoid with three principal axes $K_1 \geq K_2 \geq K_3$ (Hrouda, 1982; Borradaile, 1988). When working with igneous rocks that preserve magmatic structure, it can be shown that K_1 is parallel to the magmatic lineation and K_3 is normal to the magmatic foliation (King, 1966; Rousset and Daly, 1969; Guillet et al., 1983;

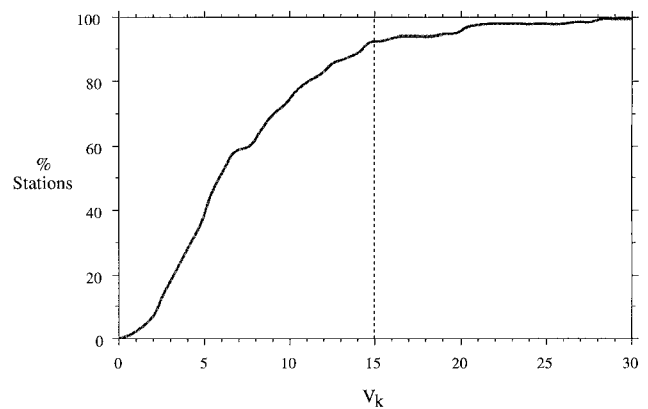


Fig. 3. Accumulated percentage of the magnetic susceptibility mean variation ($V_k\%$) values. Refer to text for explanation.

Bouchez et al., 1990; Leblanc et al., 1994; Bouchez, 1997). In the absence of solid-state deformation, the magmatic foliation represents the dynamics of the granitoid body during its ascent and/or emplacement, or the interaction of the granitoid body with the regional deformation field. This statement is valid when the fabric is acquired in the magmatic or intermediate state (Gleizes, 1992). On the other hand, the magmatic fabric can be greatly modified by solid-state deformation when strains exceed certain values (Benn et al., 1993; Benn, 1994; Bouchez and Gleizes, 1995; Riller et al., 1996).

In the study area, at least four oriented specimens were collected from each of 286 different stations (see Appendix A). AMS measurements were made with a Kappabridge susceptometer (Geofyzicka Brno) working in an alternating weak field (4×10^{-4} T, 920 Hz and a resolution better than 5×10^{-8} SI units).

5.3. Variability of the magnetic susceptibility (K)

According to Leblanc et al. (1994) the mean variation of the susceptibility (V_k) for each station is given by:

$$V_k = 100 \frac{\sum_{i=1}^n |K_i - K|}{nK}$$

where n is the number of samples and K is the arithmetic mean of the station (bulk magnetic susceptibility).

The mean V_k value for all the stations is 7.9%. According to previous studies (Leblanc et al., 1994; Román Berdiel et al., 1995), V_k values below 15% indicate that the results of sampling stations can be used without further consideration (Fig. 3). In our study, 91.8% of the sampling stations fall into this range. The 23 points with V_k values above 15% are mostly in

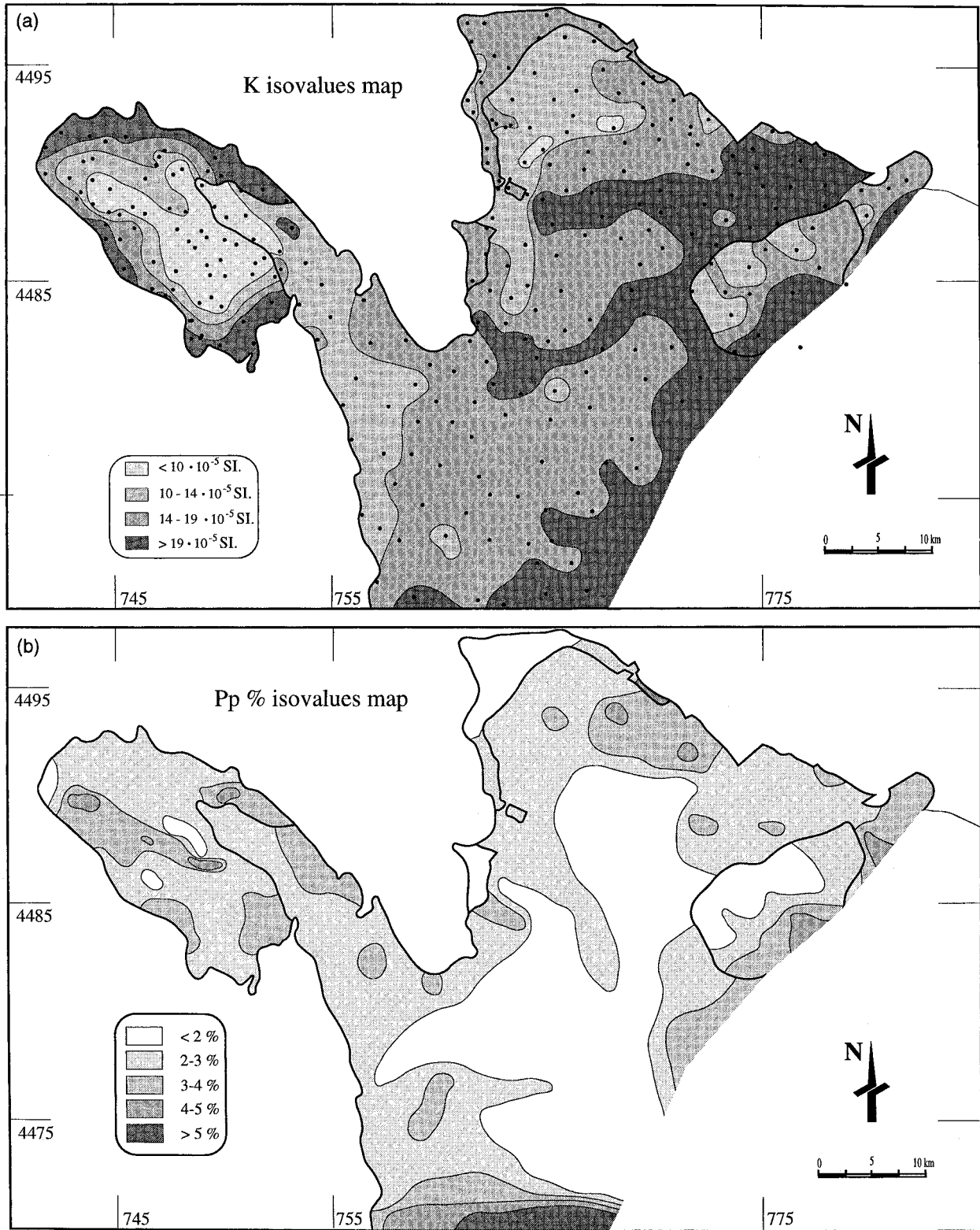


Fig. 4. (a) Isovalues map for the magnetic susceptibility (K). Black dots represent the sampling stations. (b) Isovalues map for the anisotropy degree ($P_p\%$).

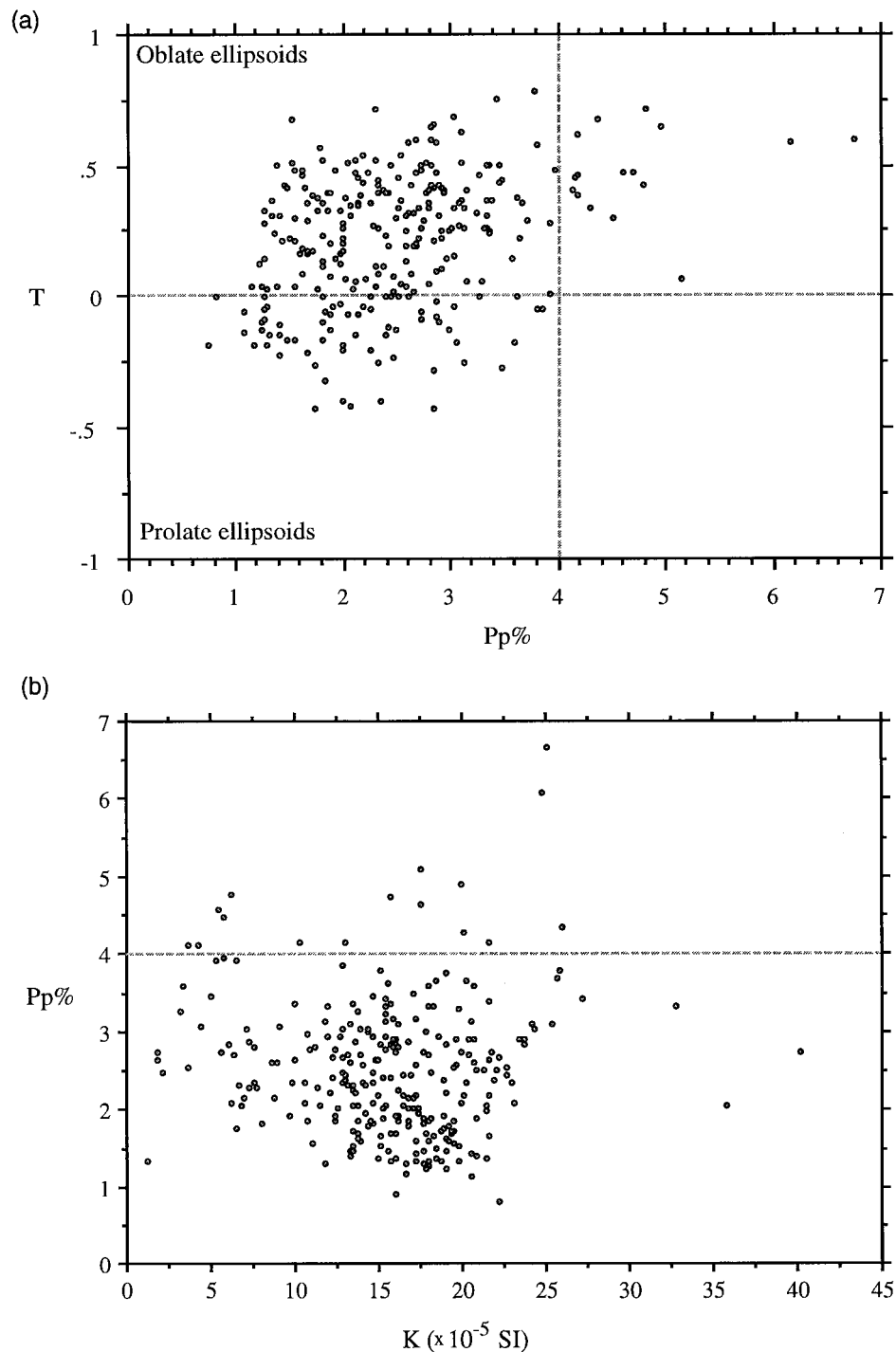


Fig. 5. (a) Anisotropy degree ($P_p\%$) vs the shape parameter (T). The magmatic ellipsoids become oblate as $P_p\%$ increases. (b) Magnetic susceptibility (K) vs anisotropy degree ($P_p\%$).

the porphyritic (19 sampling stations) and aplitic (3) facies, and one the inequigranular granite. These results indicate a large lithological influence on the susceptibility of the samples, due mainly to the presence of large feldspar crystals that lessen the susceptibility, and to biotite aggregates that, conversely, raise it.

5.4. Magnetic susceptibility (K)

The range of variation of the magnetic susceptibility (K) varies in the studied area from 1.04 and 40.2×10^{-5} SI. These values indicate a dominantly paramagnetic behavior of the granitoids (Rochette,

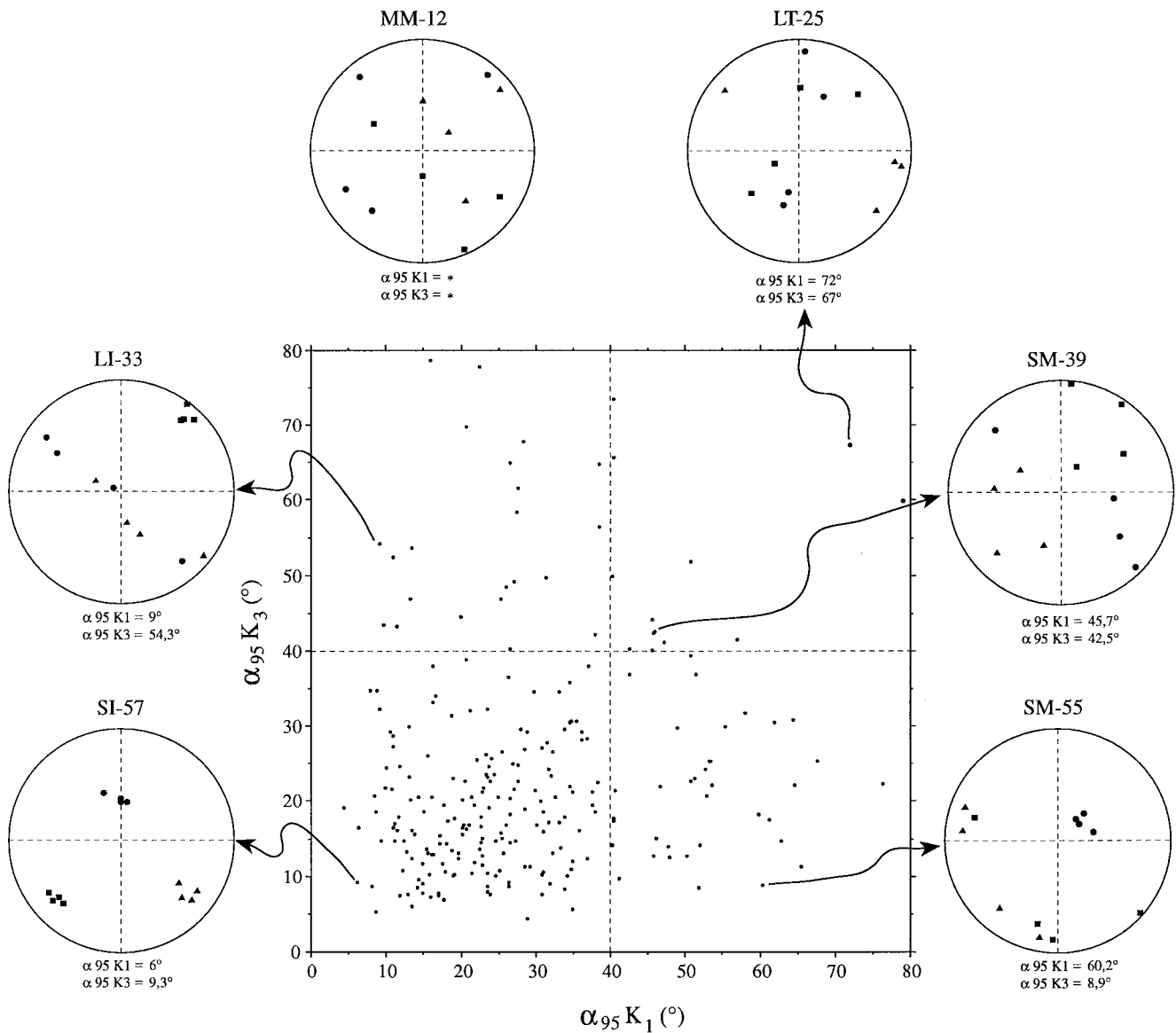


Fig. 6. α_{95} confidence cones of K_1 vs. α_{95} confidence cones of K_3 . There is a direct relation between the value of α_{95} and the rock fabric type (see text for details). Squares are K_1 ; triangles are K_2 ; circles are K_3 . The asterisks in sample MM-12 depict confidence cone values higher than those represented in the graphic.

1987). Optical microscopy indicates that biotite is the most highly represented paramagnetic mineral in these rocks, followed by muscovite, chlorite and cordierite. There is also a small isotropic diamagnetic component, produced by the quartz and feldspar content, with a constant value of -1.4×10^{-5} SI (Hrouda 1986; Rochette 1987). In these rocks, there is a direct relation between K and the weight percentage of Fe^{2+} (Rochette, 1987). Calculations result in a mean value of 1.14% Fe^{2+} for the aplitic facies, and of 2.73% Fe^{2+} for the biotitic granitoids. The latter values can be compared to the values obtained by chemical analysis (Bea et al., 1987) in the same rocks, leading to a linear relation that confirms the absence of ferromag-

netic contribution to the K value (Bouchez and Gleizes, 1995). Therefore, using the values established by Gleizes (1992), there is a close correlation between the mapped facies and bodies (Fig. 1) and the K isovalue map (Fig. 4a).

5.5. Anisotropy analysis

Previous studies (Nagata, 1961; Rochette, 1987; Bouchez et al., 1987) indicate that the anisotropy of the AMS ellipsoid is best studied through the $P_p\% = 100[\frac{(K_1 + 1.4)}{(K_3 + 1.4)} - 1]$ which includes corrections for the diamagnetic contribution of quartz and feldspar. In our study $P_p\%$ values vary from 0.72 to

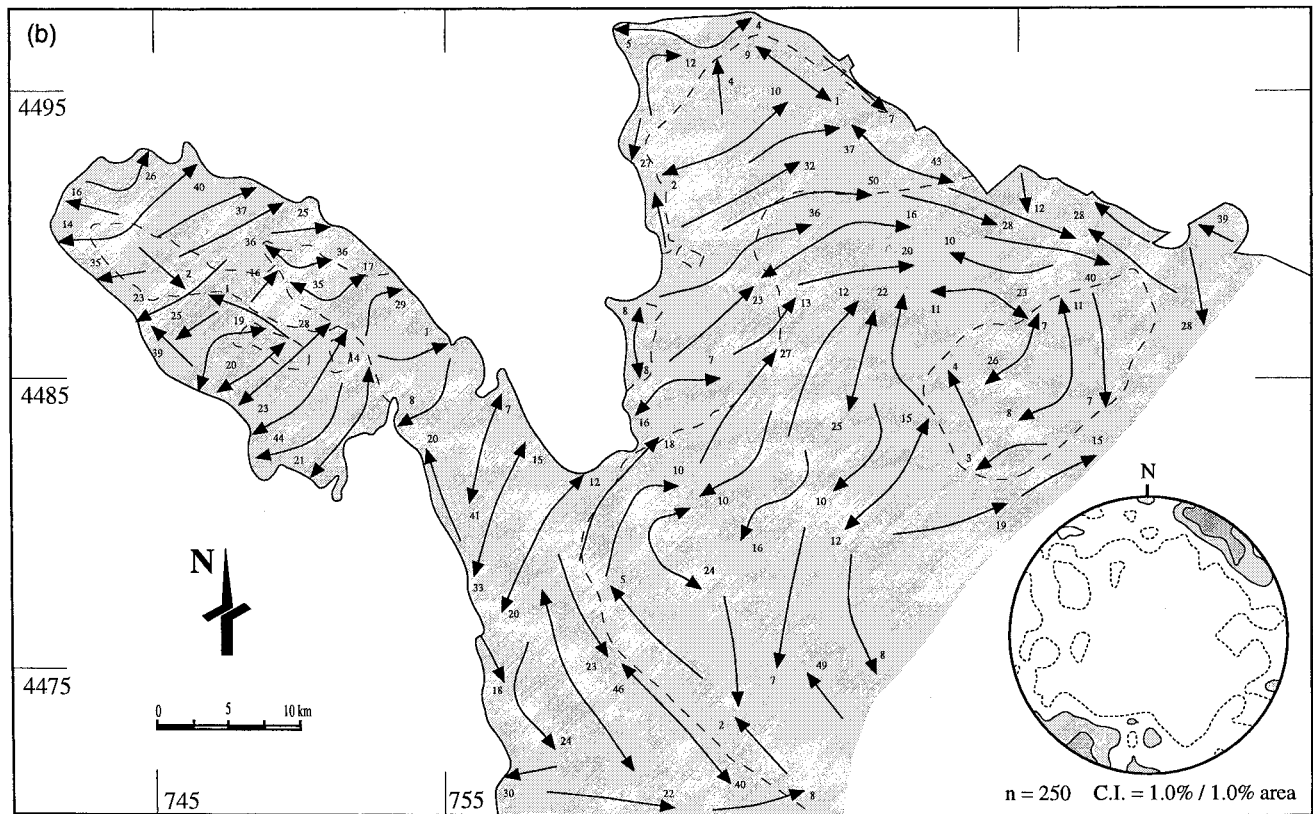
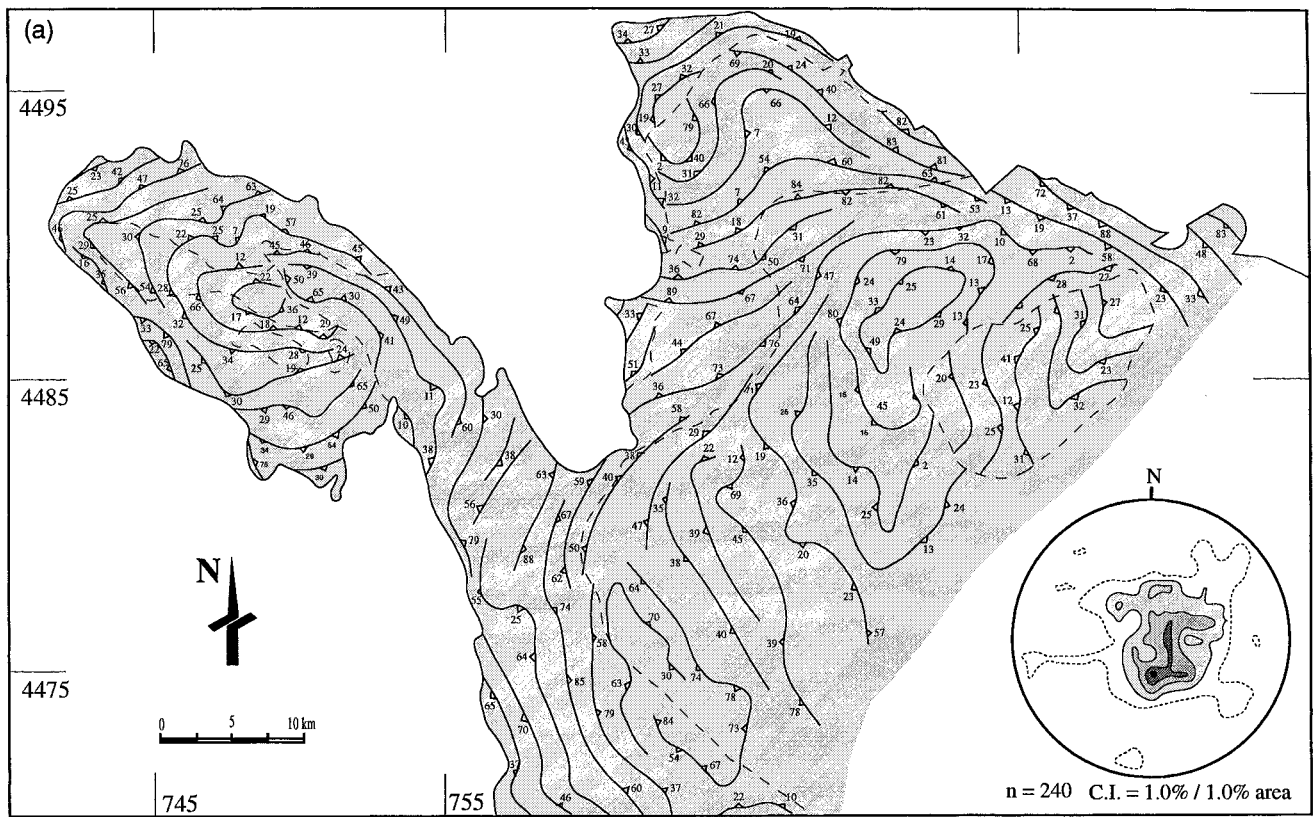


Fig. 7. (a) Magnetic foliation trace map and stereonet of the K_3 axes (Schmidt net, lower hemisphere). (b) Magnetic lineation trace map and stereonet of the K_1 axes.

6.75% with a mean value of 2.49%. These anisotropy values confirm the magmatic origin of the AMS fabric. Solid-state strain would result in much higher $P_p\%$ values. Only 5.59% of the studied samples depict tectonic AMS fabrics as they have $P_p\%$ values above 4%, and they all show an oblate shape according to the T parameter ($T = [2(\ln K_2 - \ln K_3) / (\ln K_1 - \ln K_3)] - 1$, Jelinek, 1981) (Fig. 5a) which stands in agreement with a tectonic origin (Benn, 1994). Nevertheless, in some cases the degree of anisotropy ($P_p\%$), is controlled by the mineralogy (Riller et al., 1996). In our study the samples with higher values of $P_p\%$ (>4%) do not correlate with high K values (Fig. 5b), indicating the lack of compositional control in the magnetic fabric intensity and pointing to a solid-state deformation origin.

Higher values of $P_p\%$ (Fig. 4b) are concentrated in three areas: the northern limit of the Montemayor del Río pluton, the southern part of the studied area, and the central part of the Sequeros pluton.

5.6. Variability of the directional data

The validity of the results were checked using the Fisher (1953) probability function which calculates the mean direction for each station and provides the confidence cones (α_{95}). This is one of the more common methods used to calculate the mean direction of the K tensor. Despite the fact that the principal axes of the anisotropy ellipsoid do not necessarily follow a Fisher distribution this method produces an optimum result (Ernst and Pearce, 1989; Román Berdiel et al., 1995). Other proposed methods (Tarling and Hrouda, 1993) do not include an optimum statistical treatment of the AMS ellipsoid axes orientation. According to this method, an α_{95} confidence cone is calculated for K_1 and K_3 axes. Values below 40° are considered acceptable. In this study, most of the sampling stations (80.8%) resulted in values below 40° for K_1 and even more (86.3%) for K_3 as can be seen in Fig. 6. Nevertheless, samples for which one of the values is higher than 40° can be considered because they reflect the shape of the ellipsoid. The shapes of the AMS ellipsoid can be separated into three groups illustrated in Fig. 6:

- $\alpha_{95}K_1 < 40^\circ$ and $\alpha_{95}K_3 < 40^\circ$ Planar-linear fabrics (e.g. sampling station SI-57)
- $\alpha_{95}K_1 > 40^\circ$ and $\alpha_{95}K_3 < 40^\circ$ Planar fabric (e.g. sampling station LI-33)
- $\alpha_{95}K_1 > 40^\circ$ and $\alpha_{95}K_3 > 40^\circ$ Linear fabrics (e.g. sampling station SM-55)

Stations with highly oblate (planar) ellipsoids have a great dispersion of K_1 and K_2 orientations, but they depict a good K_3 concentration which allows the use of the magnetic foliation and precludes the use of the

lineation. In contrast, highly prolate ellipsoids are characterized by a greater concentration of K_1 and dispersion of K_2 and K_3 , in which case the foliation results should not be used. In the case of 19 sampling sites with $\alpha_{95}K_1$ and $\alpha_{95}K_3$ greater than 40° the samples have been discarded, except in the case of those showing a good correlation with the neighboring measurements. The main cause of high values of $\alpha_{95}K_1$ and $\alpha_{95}K_3$ in these rocks seems to be the presence of cordierite crystals that induce a K_1 – K_3 axes inversion (Amice, 1990; sampling station LT-25), in this case there are four stations; while the high dispersion cannot be explained satisfactorily for the remaining 15 sites.

5.7. Directional data

Magnetic lineation and foliation maps were constructed (Figs. 7a and b) and although somewhat interpretative, the general fabric can be observed with much more clarity (Diot, 1989; Aranguren, 1993; Leblanc et al., 1994; Bouchez and Gleizes, 1995). Fig. 7(a) shows that the magnetic foliation is mostly sub-horizontal and strikes generally parallel to the boundaries of the plutonic bodies. In a few areas, foliation is oblique to the pluton boundaries, indicating that the granitic body probably continues below the country rock. The lineation is shallowly plunging, with trends of 020 – 050° , although some stations have trends perpendicular to this general one (Fig. 7b). Those sampling points with NW–SE lineations occur in some isolated locations in the Sequeros, Linares de Riofrío and Peromingo plutons, and in the northern and southern limits of the Montemayor del Río pluton. In all of these cases, a solid-state modification can be invoked for the anomalous trends. There is a good correlation between the areas that have NW–SE trends and those where higher degrees of anisotropy have been observed. Not all the presumably tectonically deformed rocks with $P_p\% > 4\%$ show the anomalous tectonic trend, however. The anomalous NW–SE trend is interpreted to be the result of a superposition of D_3 solid-state deformation on an original magmatic flow orientation, given that the granitoids postdate all D_2 structures. The D_3 deformation is a regional compressional event with a NE–SW shortening direction, parallel to the general trend of the magmatic lineation. The most deformed samples, therefore, should show a lineation normal to the shortening direction. However, if D_3 has affected the granitoid bodies, its influence on the AMS fabrics is only local and it does not produce sufficient finite strain to modify the original fabric (Benn, 1994). The finite strain related to D_3 is very small in the country rock and its effects are not very relevant (Diez Balda et al., 1994).

On the other hand, the Sequeros pluton has trend

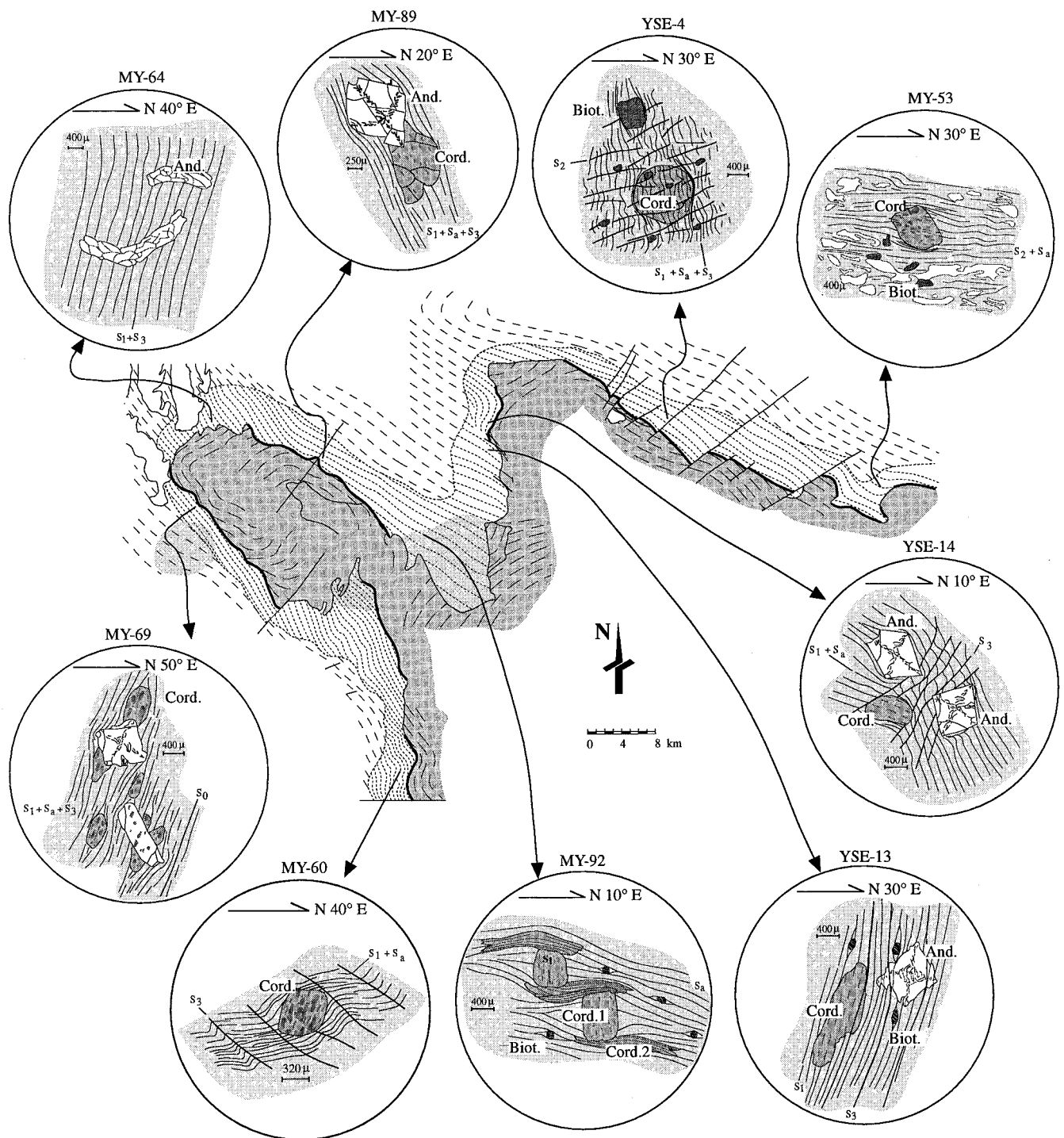


Fig. 8. Concordant contacts (in black), discordant contacts and microscopic relations between the growth of contact metamorphism minerals and the development of foliations. All the sketches are subvertical and normal to the main foliation observed in the country rock and they are represented with their original orientation. The shadowed sectors represent the areas where the ascent and/or emplacement of the magma produced crenulations. Sample MY-92 illustrates the contact metamorphism–foliation relationships. See text for details.

changes in both the azimuth and plunge of the magnetic lineation and in the dip of the magnetic foliation in its northeast and southeast limits (Fig. 7b), depicting an antiformal shape. This shape is interpreted to

be related to the magma emplacement in the core of the anticline located between the Tamames and La Peña de Francia synclines which was probably amplified under solid-state conditions during D_3 .

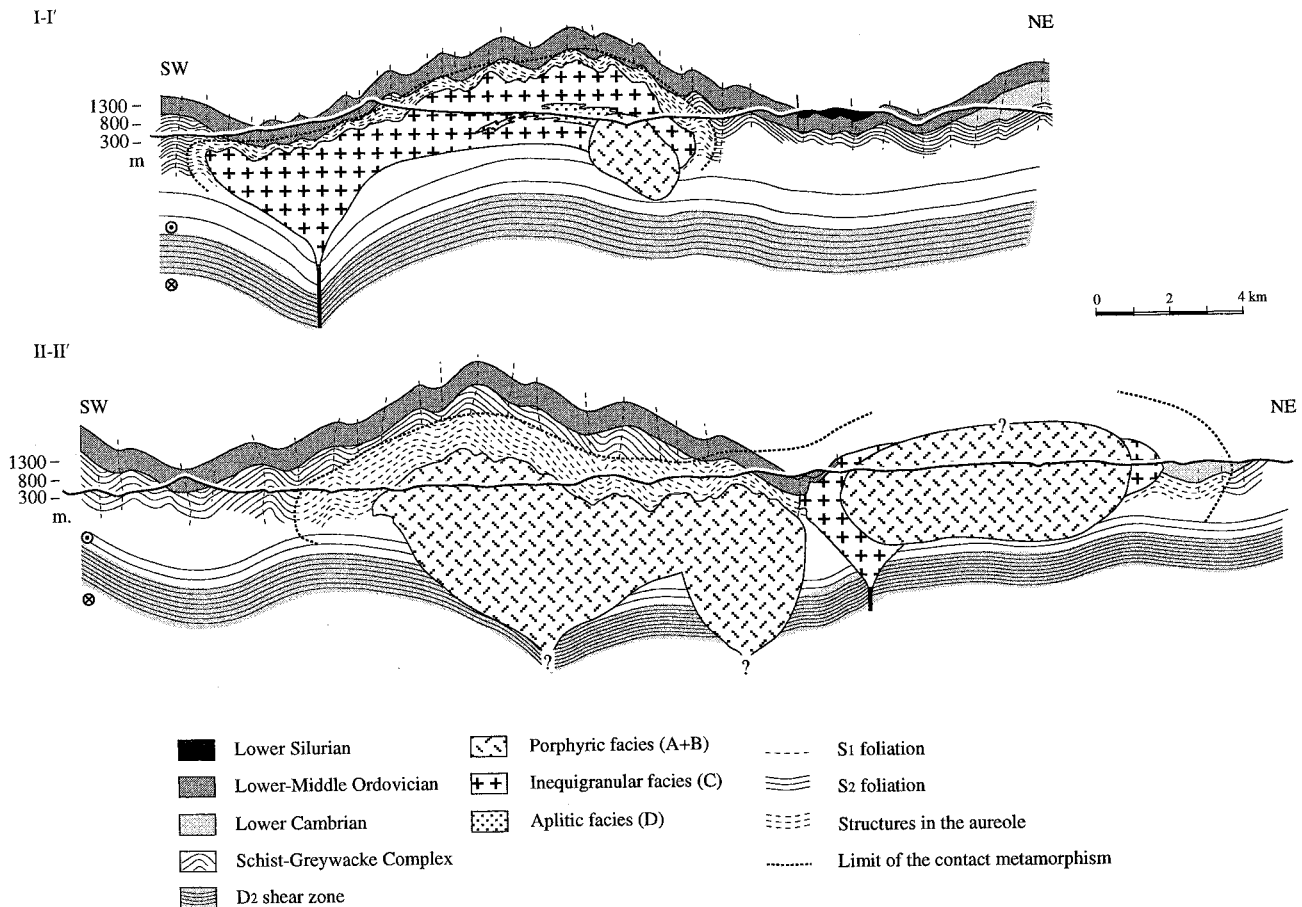


Fig. 9. Geological cross-sections of the studied area (see location in Fig. 1) built from the structural, magnetic and gravimetric data.

6. Structural study of the country rock

The emplacement of the granitoid bodies produced a contact metamorphic aureole that extends, in plan view, from 1.5 km to up to 8 km from the intrusive contacts. Pelitic rocks developed poikiloblastic cordierite crystals which are occasionally altered into pinnite. Other contact metamorphic minerals are biotite, muscovite and, locally, andalusite. Quartzites in the contact aureole develop granoblastic textures with local development of biotite.

The country rock foliation traces (S_1 or $S_1 + S_3$ or S_2), are generally oblique to the granite–country rock contact, although in some occasions they can be considered as sub-parallel (Figs. 8 and 9). This fact precludes the simple classification of these bodies into concordant or discordant plutons as suggested by Castro (1987). Concordant and discordant contacts can be present in the same pluton (Cruden, 1998), as is the case here.

At all concordant contacts (Fig. 8) there is an increase in the finite strain of the country rock towards the contact which is manifest by the parallelism of

both tectonic foliations (typically the regional foliation of the country rocks) and bedding planes to the granite contacts and the granite foliation trajectories. The higher deformation intensity in the thermal aureole can be explained either by the effects of the magma intrusion or to a later regional deformation phase (Meneilly, 1983; Lagarde et al., 1990a; Morand, 1992). Microstructures within the contact aureole at the northeast (Sample MY-89; Fig. 8) and southwest (Sample MY-69; Fig. 8) boundaries of the Sequeros pluton indicate that the temperature increase caused by this body provoked the growth of cordierite during emplacement. This was followed by andalusite growth that included the previous foliation (S_1 in this case). The foliation in the matrix is continuous showing inclusion trails in the porphyroblasts, although when observed in detail, the foliation in the matrix is also deflected around the porphyroblasts. These features can be explained either as by: (1) ductile deformation in the country rock caused by the emplacement of the Sequeros pluton re-using and re-activating (Bell, 1986; Davis, 1993) the previous regional foliation and generating a new one related to the intrusion (S_a), or (2) as

a result of D_3 deformation after pluton emplacement. Because the D_3 shortening direction is NE–SW, the structures generated during this deformation event are coaxial to those generated during D_1 and to those generated during magma emplacement. The latter precludes unambiguous explanation of the disposition of foliation.

At the northern boundary of the Montemayor del Río pluton, the main foliation is S_1 in the western part (Sample YSE-4; Fig. 8) and S_2 in the east (Sample MY-53; Fig. 8). The sub-vertical S_1 is crenulated giving rise to a new sub-horizontal S_2 crenulation cleavage. Both foliations present in the thermal aureole are approximately parallel to the granite–country rock contact and to the magnetic foliation within the pluton. Nevertheless, because of the irregular shape of the contact, it is possible to find local obliquities between country rock foliations and the intrusive contact. In the western part, cordierite postdates a vertical cleavage slightly crenulated by subhorizontal S_2 , confirming the age of the intrusion as post- D_2 . In the eastern part, cordierite grows in the micaceous domains of D_2 tectonic banding, with a mimetic disposition to the foliation. In addition, the foliation is also deflected around all the cordierite porphyroblasts. This feature could, in the western part, be partially due to the intrusion mechanism or to the D_3 event postdating the intrusion; on the other hand, in the eastern part, the sub-horizontal cleavage cannot be related to the D_3 phase and has to be related to the magma emplacement.

There are two areas where the parallelism of the structures outside and inside the granite is due to a strike change of the regional foliation. One of them is at the contact of the granite with the quartzites of the northern flank of the Tamames syncline, where S_1 and bedding change strike from NW–SE to N–S, and are parallel to the granite contact and the magnetic foliation (Sample YSE-14; Fig. 8). Ductile deformation resulting from granite intrusion probably caused a local re-orientation of the country rock structures, as well as local boudinage of the quartzite beds. The origin of this ductile deformation is interpreted to be due to the presence of a local rheological boundary, the Armorican Quartzite, as described in other sectors of the Variscan belt (Brun et al., 1990; Lagarde et al., 1990b). The impeding of magma ascent by such barrier would cause ductile deformation until the buoyancy of the magma would surpass the rheological barrier and intrude higher levels. The other area where the wall rocks have been re-oriented and the anisotropy planes parallel the granitoid boundary is in the western contact of the Montemayor del Río pluton (Sample MY-60; Fig. 8).

The latter two areas reflect the role of D_3 , as the pre-existing foliation is not normal to the shortening

direction of this deformation phase. Sample YSE-14 depicts some crenulation of S_1 , concentrated in bands. In sample MY-60, D_3 rotates the foliation around the porphyroblasts, producing a high angle between the matrix cleavage and that included in the porphyroblasts.

In contrast to the concordant contacts, the discordant contacts (Fig. 8) are very irregular, with interdigitations with the country rock produced by magma injection sometimes parallel to S_1 and sometimes parallel to other anisotropies, usually bedding. Some outcrops show large blocks of country rock within the granitoid mass indicating local stoping processes. Contact metamorphic minerals post-date D_1 and cuts S_1 cleavage (Sample MY-64, Fig. 8), although in some cases it is mimetic (Sample YSE-13, Fig. 8). However, they do not have any preferred orientation on S_1 planes. No re-working or re-flattening of S_1 has been observed which means that no ductile deformation in the country rock is related to the emplacement of the granitoids in the discordant contacts. This is common in the discordant plutons, in which the country rock plays a passive role during the intrusion without undergoing deformation (Castro, 1987). D_3 deformation can be recognized in some thin sections collected in these contacts. In sample MY-64 (Fig. 8) the main foliation (N130°/80°SW) is oblique to the granite contact (approximately N–S) and prismatic andalusite crystals grow across S_1 , but with the long axes parallel to the granite contact. The andalusite crystals were subsequently shortened during D_3 . In sample YSE-13 (Fig. 8) some S_3 pressure solution cleavage apparently cut the andalusite crystals and are parallel to S_1 .

The effect of D_3 in the country rocks outside the thermal aureole is negligible (Diez Balda et al., 1994), whereas inside the aureole development of structures is favored by what we interpret as strain softening caused by the temperature increase (Pitcher and Berger, 1972; Sanderson and Meneilly, 1981; Meneilly, 1982; Bateman, 1985; Lagarde et al., 1990a; Brun et al., 1990).

6.1. Magma emplacement related crenulations

Evidence for deformation of the country rocks related to magma emplacement exists as crenulating of pre-existing foliation planes (Fig. 8). For example, in sample MY-92 (Fig. 8) two cleavages can be observed: a vertical one striking NW–SE (S_1) and another shallow dipping to the east. Two generations of cordierite porphyroblasts can be distinguished: (i) those that contain the S_1 cleavage, some of which are a little elongated parallel to those planes, due to a mimetic growth or a slight re-flattening during emplacement; (ii) cordierites that grew simultaneously to the development of the sub-horizontal foliation, which are

strongly elongated and have an internal cleavage parallel to that in the matrix (sub-horizontal), which is slightly re-flattened around the cordierite porphyroblasts.

We interpret that the first generation of cordierite crystals is caused by the intrusion of the Sequeros and Linares de Riofrío plutons. Subsequently, the intrusion of the Montemayor del Río pluton would cause the horizontal crenulation and the simultaneous development of the second generation of cordierite crystals. Analogous situations have been described in Donegal (Ireland) by Smart (1962) and Pitcher and Berger (1972) where the growth of two generations of andalusites with different habits is interpreted to correspond to the different thermal response to two discrete magmatic pulses.

The most intense strain related to the pluton intrusion occurs close to the top of the Montemayor del Río pluton. Analog models of diapiric granite emplacement (Ramberg, 1981) predict that ductile deformation in the country rock is most intense at the top of the pluton (Schwerdtner, 1995). Furthermore, other models, such as expansion (Guglielmo, 1993b), predict superposition of structures, including the development of composite fabrics such as the crenulation cleavages described above.

7. Model of emplacement: discussion and conclusions

One of the main objectives of this study was to construct cross-sections of the granitoid bodies and the country rock, in order to develop an emplacement model. Such cross-sections were constructed normal to the main Variscan structures using all the available geological data, together with the AMS data and the gravity modeling results; in addition, a possible continuation of the D_2 shear zones has been added (Fig. 9). In the cross-sections the Sequeros pluton is interpreted to have a sheet-like shape (average 2 km thick) that is concordant with regional scale folds (e.g. cross-section I–I', Fig. 9). Magma emplacement is interpreted to have taken place from a 'root zone' located in the southwest and magma flowed to the northeast into the core of the D_1 anticline located between the La Peña de Francia and Tamames synclines. The top of the intrusion is very close to the bottom of the Armorican Quartzite Formation, but is never in contact with it. The bottom of the intrusion is probably controlled by the sub-horizontal anisotropy related to the D_2 shear zones. A similar geometry can also be inferred for the Linares de Riofrío pluton (cross-section II–II', Fig. 9), although it is difficult to prove because it is obscured by the later Montemayor del Río intrusion. The Linares de Riofrío pluton cuts the Armorican Quartzite Formation. The geometry of the

Montemayor del Río pluton resembles an inverted drop. It is larger than the others and has a deeper root and the lower walls are inferred to be much steeper (cross-section II–II', Fig. 9). This tabular shape, with horizontal dimensions much larger than vertical dimensions (Hamilton and Myers, 1967; Myers, 1975; Vigneresse, 1995; McCaffrey and Petford, 1997; Cruden, 1998) and shallow dipping floors towards one or two root-zones (Brisbin and Green, 1980; Evans et al., 1994; Vigneresse, 1995; Dehls et al., 1997; Cruden, 1998) is commonly described.

In this region of the Variscan belt (the Central Iberian Zone) it is believed that the ascent and emplacement of the plutons took place after D_2 extensional collapse and during the D_3 compressive stage. D_1 thickening raised the lower crust temperature and the decompression produced during subsequent orogenic collapse triggered partial melting (Dewey, 1988; Speer et al., 1994). The ascent of granitic melts from the generation zone to the epizonal levels where the emplacement took place is not thought to occur diapirically in cold and brittle country rock (Marsh, 1982; Daly and Raefsky, 1985; Brun et al., 1990; Schmidt et al., 1990). In the study area, magma ascent took place in a compressive regime (D_3), in which case the opening of conduits for the magma could only take place by reactivation of sub-vertical NE–SW normal faults or fractures generated during the D_2 extensional stage. These fractures would be parallel to σ_1 during D_3 , allowing tensile opening and magma transport to higher levels in the crust. This mechanism of fracture development, postulated by Anderson (1951), has been used by several authors to explain magma ascent from deep zones (Shaw, 1980; Castro, 1987; Brun et al., 1990; Clemens and Mawer, 1992; Parsons et al., 1992; Petford, 1996).

Upon reaching the emplacement level, mechanisms of final emplacement often invoke the existence of large active structures during the emplacement that would provide enough room for the magma. These models include pull-aparts (Guineberteau et al., 1987; Schmidt et al., 1990; Lagarde et al., 1990a; Morand, 1992; Archanjo et al., 1994; Evans et al., 1997), large tension gashes (Castro, 1987) and shear zone terminations (Hutton, 1988; Lagarde et al., 1990b; Amice, 1990; Ferré et al., 1995). Other models propose lateral expansion of the magma when a rheological barrier is reached (Bateman, 1985; Brun et al., 1990; Lagarde et al., 1990b; Román Berdiel, 1994). However, the latter does not fully solve the room problem, because ductile deformation can only explain the 40% of the required space (Paterson and Fowler, 1993). This objection is also relevant in this study where very little ductile deformation has been observed in the country rock along the concordant margins and near the roof of the pluton.

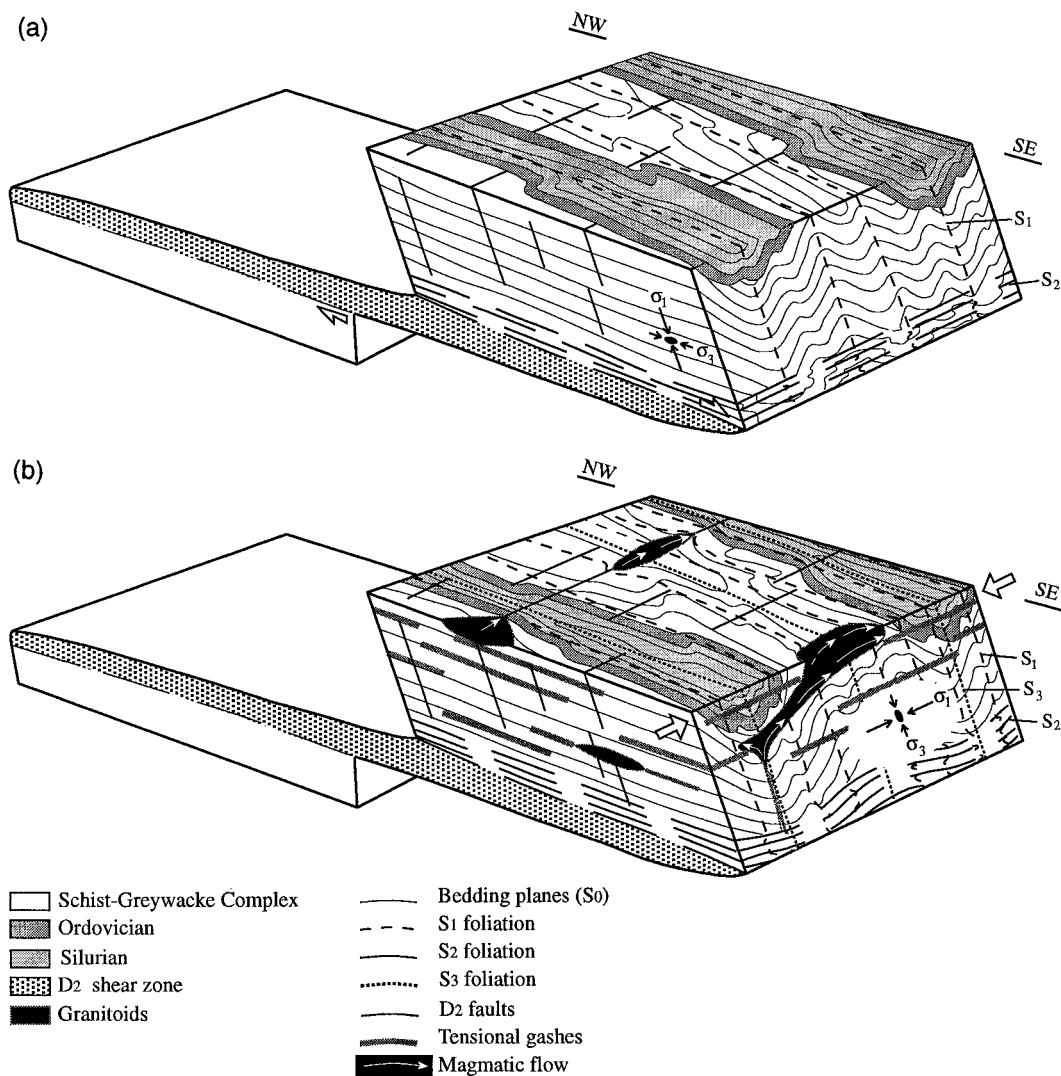


Fig. 10. (a) Structures developed in the area during the early stages of the Variscan deformation (D_1 and D_2 , modified from Díez Balda et al., 1994). Note how in the shear zone hanging wall fractures parallel to σ_1 during D_2 are developed. (b) Structural sketch depicting the magma ascent through the fractures developed and its emplacement in sub-horizontal levels parallel to σ_1 during D_3 . There is additional control related to the involved lithologies and the folds in the country rock. Emplacement room is generated by floor depression.

The absence of large structures related to the granitoids in this study and the lack of ductile deformation in the country rock requires that the emplacement mechanism be a combined effect between the regional stress field and the magma buoyancy, as invoked by Hutton (1988) and Parsons et al. (1992). D_3 acted with the maximum compressive stress (σ_1) sub-horizontal and directed NE–SW (Fig. 10). In the upper level of the crust, σ_3 was vertical, which would result in horizontal tension fractures according to an Andersonian fracture system. The horizontal fractures would host the magma as sheet shaped bodies (sills, laccoliths or lopoliths). The magma flow, from the AMS studies, is parallel to the σ_1 direction, as in other plutons emplaced in a compressional environment (Brun and

Pons, 1981; Román Berdiel, 1994) and opposite to the ones studied by Brun et al. (1990).

There is a rheological control of the emplacement level which can be correlated with several features: (1) the presence of the Armorican Quartzite Formation which act as a rheological barrier, despite it being cut by some of the plutons; (2) the presence of sub-horizontal discontinuities (mostly bedding and S_2 in deeper levels) favors fracture generation (Clemens and Mawer, 1992; Cook and Gordon, 1964) and; (3) the D_1 antiform cores mediate magma migration from roots located in the synclines.

The latter elements can be integrated into an emplacement model for the La Alberca–Béjar granitoids. Initially, the space necessary for granitoid emplace-

ment was created by tectonic processes (tension fractures), but the deformation within the magma mass was controlled by the igneous processes as proposed by Guglielmo (1993a) for the Merrimac pluton. Therefore, the flow of magma should be controlled by the (a) geometry of the space being created (b) by the magma buoyancy and (c) the presence of different magmatic intrusion phases allowing the magma to be emplaced by flow parallel to the main compressive stress. Hutton (1992) postulated that in these cases there is no need for tectonic dilation when there is enough magma to generate the room by wedging, even in compressive regimes. Once the first plutons had been emplaced, the Montemayor del Río pluton would follow, using the same mechanisms followed by the Linares de Riofrío and the Sequeros bodies. The intrusion of the first plutons would have eased introduction of the later bodies by generating a ‘thermally prepared zone’ (Marsh, 1982; Mahon et al., 1988; England, 1990; Davis, 1993).

The room needed to accommodate the large amounts of magma involved in these granitoid bodies should be produced by several mechanisms acting simultaneously: tectonic dilation; some ductile deformation in the country rock, mostly in the concordant contacts and in the pluton roof; stoping; and floor displacement that would contribute greatly to the room generation. We believe that floor depression is the most important mechanism for generating sufficient room for these intrusions. This conclusion is reached

from the data interpretation presented in this work and the geometry of the metamorphic country rock and the plutons (Fig. 9). In addition, there is no evidence of roof-lifting in the structures present above the studied granitoid bodies. From this point of view the ‘cantilever model’ (Cruden, 1998) could be the most appropriate to explain the La Albea–Béjar plutons as it does not require the presence of structures close to the surface related to the room generation. This intrusion mechanism does not preclude the operation of other ones (see Cruden, 1998, for a detailed discussion).

The last recognized effect, once the plutons have intruded, and while the D_3 compressive conditions prevail, is the generation of the solid-state deformation observed in the granites and the country rocks. The magnetic lineations obtained in some samples would be caused by these late movements.

Acknowledgements

We wish to thank J.L. Vignerese, J.L. Bouchez, G. Draper, D.G.A.M. Aerden, H. Koyi and the Structural Geology Working Group at Salamanca University for the critical input and very helpful discussions. A.R. Cruden and D.B. Clarke significantly streamlined the text. This work has been funded by DGICYT through grant PB-96-1452-C03-02.

Appendix A. Results from the sampling stations

X, Y: UTM units. dK_1 , dK_3 : azimuth of K_1 and K_3 . iK_1 , iK_3 : plunge of K_1 and K_3 . K : mean magnetic susceptibility (in 10^{-5} S.I.). $P_p\%$: anisotropy degree. $95(K_1)$: confidence cone (α_{95}) for K_1 axes. $95(K_3)$: confidence cone (α_{95}) for K_3 axes. V_k : mean variation of the susceptibility.

Table A1

No.	X	Y	dK_1	iK_1	dK_3	iK_3	K	$P_p\%$	$95(K_1)$	$95(K_3)$	V_k	No.	X	Y	dK_1	iK_1	dK_3	iK_3	K	$P_p\%$	$95(K_1)$	$95(K_3)$	V_k
1	744.00	4489.79	208	24	62	60	9.49	1.86	25.4	26.7	3	87	762.27	4492.14	65	12	261	79	12.18	2.38	38.3	22.5	14.6
2	743.56	4489.08	199	19	63	64	13.13	3.08	15.5	13.2	6.05	88	763.44	4493.56	322	5	53	11	13.38	1.98	27.9	29.7	5.23
3	744.86	4489.38	*	*	251	78	5.57	3.96	*	*	74.7	89	761.18	4496.10	88	4	181	57	15.40	1.38	40.4	17.5	8.95
4	746.81	4490.11	89	24	240	65	15.29	2.74	33.2	13.9	17.4	90	765.17	4490.58	50	4	153	72	17.02	3.47	10	24.6	4.18
5	745.25	4488.14	263	26	55	62	12.58	2.91	30.7	27.2	2.66	91	764.83	4491.28	244	3	160	84	9.67	2.29	29.6	34.6	10.6
6	743.92	4488.65	249	43	43	44	9.83	3.35	30.8	10.4	2.98	92	761.97	4490.98	320	10	211	58	14.82	2.12	30.6	20.1	4.12
7	746.33	4489.44	66	2	157	68	13.56	2.84	23.6	19.2	4.9	93	764.89	4488.97	62	62	192	16	20.02	2.12	23.8	22.8	14.7
8	742.59	4492.02	85	11	330	67	40.20	2.71	14.8	7.8	12.8	94	765.68	4489.40	51	1	319	40	18.59	1.66	16	12.9	6.13
9	741.93	4491.32	*	*	166	65	35.74	1.99	*	17.6	5.3	95	766.79	4490.28	102	36	*	*	15.00	1.60	20.7	69.9	7.8
10	744.73	4491.56	36	36	144	23	17.92	2.68	12.9	30	2.37	96	768.65	4491.58	98	50	359	8	19.44	1.50	31	18.7	10.0
11	744.02	4490.81	*	*	*	*	13.40	2.19	*	*	5.74	97	766.00	4492.08	43	32	161	36	11.89	2.90	36.8	28.4	5.97
12	741.58	4489.96	200	35	73	44	17.11	1.53	23.3	26.4	4.23	98	766.93	4491.12	81	40	178	6	17.02	1.97	32	23.4	4.26
13	748.22	4491.33	42	37	162	27	20.32	6.15	27.6	22.7	3.31	99	768.19	4492.21	*	*	*	*	8.90	3.06	72	67	10.6
14	747.18	4490.68	219	6	120	26	18.45	2.92	38.4	56.5	1.81	100	765.43	4493.54	37	3	248	83	13.59	3.26	45.7	12.8	6.15
15	749.77	4490.84	171	7	284	73	21.99	2.47	33.8	8.3	3.59	101	766.23	4492.84	56	24	318	14	12.66	2.45	10.8	27.3	5.27
16	751.88	4489.43	14	40	218	45	24.10	3.07	22.4	77.9	12.1	102	769.95	4492.40	266	52	20	19	15.78	3.13	34.9	12.1	8.83
17	749.99	4489.94	78	25	193	44	21.44	4.17	29.2	11.4	1.7	103	768.41	4493.87	77	33	221	57	19.82	4.95	20.5	22.8	15.5
18	751.44	4486.75	5	14	138	65	6.58	2.28	*	25.9	10.1	104	769.62	4494.31	134	7	39	30	14.48	2.04	16	20.6	8.51
19	750.62	4486.88	36	28	202	61	7.64	2.23	11.7	7.4	5.52	105	771.02	4493.59	317	55	215	8	15.88	2.82	12.6	13.3	19.4
20	749.79	4487.19	51	14	233	78	5.30	4.59	28.5	19	8.16	106	769.68	4493.39	4	40	261	18	13.80	3.01	12.9	23.3	7.97
21	749.72	4485.66	221	26	25	62	4.81	3.45	33	34.6	24.2	107	766.43	4493.98	41	10	*	*	12.85	2.34	9	54.3	11.2
22	748.34	4488.44	40	16	179	68	10.66	2.95	15.2	13.7	1.69	108	767.64	4495.02	337	10	236	50	15.80	2.78	23.5	10.5	6.33
23	747.62	4488.49	340	20	181	78	10.88	1.48	61.1	17.6	6.93	109	762.12	4497.12	22	12	143	63	15.82	2.83	46.1	15.2	1.56
24	747.95	4487.52	289	1	20	73	2.98	3.25	27	21.7	6.17	110	761.42	4497.08	274	5	178	56	17.88	1.78	22.8	11.5	5.81
25	748.96	4486.95	297	12	175	72	6.11	4.80	25.6	13.2	2.56	111	767.31	4496.88	71	14	208	71	17.88	1.78	23.8	7.6	4.57
26	748.66	4486.64	92	19	320	63	5.12	3.92	12.2	14.8	6.31	112	766.62	4495.66	332	9	203	70	12.22	1.78	59.7	18.4	6.68
27	747.74	4486.37	179	34	4	56	4.05	4.14	23.5	8	13.5	113	765.87	4496.47	340	23	206	66	13.30	1.37	50.7	52	47.8
28	747.91	4485.61	339	15	85	49	1.61	2.70	*	35.6	0.12	114	765.04	4497.57	14	4	125	69	15.99	1.86	27.2	14.7	2.09
29	748.86	4485.78	12	25	111	18	6.41	3.92	9.7	21.8	3.57	115	763.39	4492.35	258	2	167	59	12.72	3.02	33.7	17.9	8.17
30	748.66	4484.11	*	*	*	*	8.69	2.10	*	*	6.16	116	764.05	4490.72	54	8	148	8	7.41	2.30	13.3	53.7	35.7
31	749.01	4482.57	245	60	26	25	21.50	3.38	17.9	14.4	2.44	117	762.36	4488.96	51	16	190	71	10.43	2.31	14.2	20.6	14.1
32	751.34	4482.08	*	*	346	60	20.82	1.31	55.2	30	4.24	118	770.86	4492.73	298	37	203	7	15.28	3.11	15.6	10.4	3.03
33	750.99	4483.36	204	32	334	36	32.67	3.32	27.1	49.2	9.23	119	771.71	4492.18	92	43	193	9	17.46	4.68	16.2	38.1	6.19
34	752.33	4484.20	197	19	301	40	20.82	2.46	18.7	31.5	4.16	120	772.12	4491.50	114	4	24	29	17.86	1.20	24.4	23.6	3.65
35	752.47	4485.37	11	10	134	67	11.76	3.33	8.7	34.8	11.4	121	772.77	4490.34	95	26	332	58	18.84	2.35	20.6	39	12.5
36	751.39	4485.24	192	35	299	25	7.01	3.02	28.3	68	7.66	122	773.63	4489.10	280	10	64	73	21.54	2.61	21.3	20.7	4
37	749.83	4483.68	358	13	242	43	8.47	2.57	45.5	44.2	21.9	123	773.78	4491.03	115	16	13	37	22.10	2.63	18.7	13.5	1.02
38	751.86	4486.26	28	14	137	54	8.85	2.57	14.2	9.6	10.6	124	775.75	4492.50	223	69	50	18	18.98	3.77	22.5	14.5	6.01
39	743.18	4488.63	250	35	73	55	3.13	3.60	18.8	10.1	9.7	125	774.64	4491.24	194	12	44	77	20.09	2.31	30.9	10.7	6.5
40	744.38	4487.52	225	28	8	57	20.54	3.57	24.6	10.1	5.32	126	774.02	4490.06	257	10	70	80	22.90	2.29	19	17.7	10.1
41	746.04	4487.66	225	25	66	58	15.35	3.22	13.3	16.2	6.5	127	772.37	4492.56	50	46	194	38	12.66	3.84	11.5	17.9	11.4
42	745.56	4485.68	302	39	55	25	21.72	2.72	52.6	24.3	8.48	128	775.16	4489.62	96	40	348	22	21.29	1.92	22.1	25.6	13.6
43	746.94	4486.04	*	*	*	*	13.20	2.57	*	*	4.17	129	777.95	4491.11	317	23	48	2	20.50	3.11	19	10.3	8.75
44	747.75	4484.75	209	6	111	59	13.23	2.56	45.6	40.1	4.9	130	776.82	4490.87	127	0	30	53	21.85	2.35	23	21.8	9.89
45	744.35	4486.92	*	*	*	*	19.51	2.52	*	*	3.54	131	774.84	4490.47	107	-2	12	71	19.40	2.49	26.5	14.5	10.6
46	744.01	4491.80	10	26	126	48	20.62	2.86	23.6	24.7	3.87	132	772.41	4488.75	21	18	193	76	24.22	3.02	51.7	8.5	6.27
47	745.43	4491.86	55	40	156	14	20.23	2.67	13.3	12.5	2.59	133	770.44	4488.40	51	11	304	65	20.74	1.83	48.9	29.9	14.8
48	747.79	4490.04	16	7	128	83	5.40	2.69	30.1	16.9	10.9	134	769.80	4487.57	344	32	153	57	15.19	2.38	22.6	18	7.5
49	748.99	4489.54	328	36	180	45	3.46	2.50	56.9	41.6	8.61	135	768.54	4487.21	28	12	117	10	18.87	1.54	13.2	46.9	6.6
50	742.82	4489.86	273	14	32	61	10.18	4.16	*	*	20.6	136	770.29	4491.70	19	82	185	7	15.02	3.80	21.6	12	2.31
51	746.37	4488.10	214	52	*	*	3.55	4.13	15.8	78.7	2.68	137	771.64	4490.62	131	16	352	67	18.90	1.39	16.2	13	12.5
52	745.36	4487.10	305	28	40	11	17.93	3.32	50.7	22.8	5.45	138	767.62	4488.22	91	38	290	47	22.18	0.72	26.4	40.3	10.7
53	748.03	4482.48	*	*	256	5	21.48	2.12	*	*	4.8	139	766.82	4487.34	0	43	122	26	18.01	1.82	35.3	30.8	6.62
54	747.37	4483.18	253	23	26	56	17.78	2.97	19.5	12.5	5.81	140	777.97	4489.63	303	28	58	32	21.59	1.58	45.8	42.6	9.7
55	746.54	4484.14	227	20	357	60	19.70	3.28	6	9.3	2.7	141	768.64	4490.33	28	11	252	76	18.72	1.86	11.1	17.1	9.04
56	751.52	4485.92	306	20	154	66	5.86	2.80	16.8	7.4	1.02	142	767.12										

173	774.53	4485.85	235	26	105	49	13.11	1.32	21.7	19.5	6.6	260	762.90	4489.00	71	13	190	54	20.26	2.86	34.7	30.8	10.1		
174	776.67	4486.67	355	11	112	59	13.60	1.62	34.8	21.3	1.45	261	762.00	4487.10	0	8	103	57	17.20	1.90	20	16.5	5.51		
176	780.94	4489.51	169	28	48	42	17.93	3.58	35.8	16.1	7.25	262	766.20	4472.30	324	2	225	26	17.77	1.63	67.6	25.4	4.83		
177	779.89	4488.34	308	7	54	67	12.88	4.16	13.3	6	20.1	263	765.00	4470.70	48	16	182	68	24.95	6.75	21.4	10.5	11.7		
178	778.03	4488.72	208	9	324	68	23.27	2.88	34.9	5.7	4.79	264	766.60	4470.70	67	8	218	80	29.41	7.45	8.5	5.4	5.43		
179	777.81	4485.85	168	9	70	50	15.56	1.25	29.8	21.5	10.9	265	763.30	4469.90	109	32	256	53	24.76	6.14	13.6	15.7	1.66		
180	776.56	4484.70	231	8	334	58	25.94	4.36	4.3	19.2	4.33	266	756.90	4471.60	260	30	114	53	14.49	2.42	31.6	24.3	3.21		
181	774.89	4482.79	278	30	74	59	27.18	3.43	22.7	21.3	4.51	267	744.50	4489.90	209	12	92	59	13.30	1.65	23.4	23.3	1.94		
182	773.48	4481.62	225	3	123	76	25.74	3.79	9.2	14.8	3.8	268	750.30	4488.60	124	19	359	51	11.29	1.99	38.4	64.8	3.46		
183	773.69	4483.66	346	22	137	65	13.26	1.44	40.3	17.7	3.92	269	750.40	4488.50	325	0	208	64	4.29	3.03	11.4	43.4	10.0		
184	772.17	4480.80	70	19	285	66	21.14	2.47	9.1	32.3	28.2	270	749.10	4487.50	38	16	293	54	6.30	1.70	51.3	37	12.9		
185	771.41	4479.65	103	11	323	77	25.62	3.70	17.5	11.7	20	271	748.90	4485.80	*	*	*	*	7.40	2.77	*	*	5.65		
186	769.67	4480.66	222	15	102	65	15.54	1.61	26.8	25.1	3.17	272	753.00	4484.10	248	8	36	80	12.20	1.86	9.6	43.5	14.0		
187	770.90	4482.18	*	*	*	*	16.94	2.10	*	*	3.39	273	756.40	4474.40	144	18	47	25	13.51	2.17	31.7	17.3	17.2		
188	769.22	4476.58	157	8	252	33	16.72	1.95	10.5	29.4	5.04	274	759.00	4470.60	111	10	213	44	20.06	4.29	30.8	7.7	5.47		
189	767.22	4474.63	311	49	45	12	18.58	1.26	34.5	35.9	2.65	275	762.00	4470.50	120	22	223	30	17.40	5.13	7.9	34.8	1.69		
190	765.00	4474.61	172	77	13	12	19.06	1.72	14.9	18.6	10.4	276	781.30	4488.50	173	8	69	57	21.37	1.99	34.6	11.1	4.09		
191	763.68	4475.29	326	25	65	16	18.40	1.42	40.1	50	3.3	277	744.73	4490.32	*	*	*	*	1.04	1.24	*	*	10.4		
192	764.84	4476.88	162	4	64	50	16.96	2.09	20.2	16.9	6.13	278	748.66	4487.52	325	21	128	65	6.84	2.09	25.4	15.2	2.42		
193	765.23	4478.84	325	9	233	1	16.49	1.07	32.2	26.7	5.44	279	747.91	4485.61	236	4	133	71	5.66	4.50	14.7	11.8	2.74		
194	767.08	4479.41	218	13	353	65	15.07	1.47	53.1	25.4	3.97	280	771.70	4491.90	100	8	279	82	2.97	5.92	28.8	4.4	1.18		
195	768.99	4478.01	182	19	48	67	18.26	1.28	23.3	23.7	6.63	281	769.90	4494.70	*	*	226	78	1.05	2.90	*	47.5	6.22		
196	764.30	4471.93	153	40	260	23	19.91	2.04	51.9	14.2	15.7	282	769.90	4494.70	135	3	245	62	1.95	1.81	*	*	41.9		
197	765.27	4473.25	*	*	*	*	19.03	1.53	*	*	4.63	283	763.00	4492.50	68	2	166	68	0.40	2.25	*	20.8	17.5		
198	767.56	4476.88	210	12	24	78	19.34	1.80	*	*	9.18	284	769.90	4494.70	96	11	350	57	16.38	2.39	10.8	16.5	5.25		
199	766.56	4475.49	193	7	85	51	17.58	1.38	27.6	61.7	2.4	285	762.90	4492.60	217	1	24	88	15.99	2.21	37.6	21.3	8.29		
200	762.18	4475.14	180	24	*	*	15.88	1.87	25.2	47	8.67	286	744.73	4490.32	15	5	164	78	12.69	2.30	25.9	48.5	7.84		
201	763.43	4472.89	291	1	20	36	16.11	1.79	21.1	32.2	9.28														
202	762.16	4487.85	83	43	180	1	12.95	2.40	28.5	27.1	20.6														
203	761.21	4486.78	30	4	119	16	1.67	0.98	26	27.2	20.3														
204	761.99	4486.22	163	8	7	81	14.07	1.89	21	16.9	2.9														
205	761.45	4485.16	*	*	154	39	17.14	1.36	58	31.8	4.64														
206	763.39	4484.48	350	26	204	56	11.63	3.11	24.8	20.7	20.5														
207	764.57	4483.84	*	*	*	*	16.40	1.99	*	*	11.7														
208	765.09	4482.35	176	3	84	78	17.07	1.25	40.6	21.6	8.71														
209	764.65	4481.60	260	10	*	*	19.77	1.24	26	48.6	4.11														
210	763.87	4479.98	183	16	71	51	19.24	1.66	34.4	30.6	3.77														
211	763.15	4479.02	*	*	*	*	18.13	1.60	*	*	12.6														
212	760.74	4478.69	*	*	*	*	15.93	0.81	*	*	15.0														
213	758.82	4477.20	*	*	*	*	14.42	1.79	*	*	5.15														
214	757.53	4477.20	204	20	356	65	12.45	1.97	28.8	29.4	4.08														
215	759.95	4479.64	17	3	110	42	15.97	1.27	41.1	9.8	13.8														
216	753.78	4486.06	68	0	116	82	13.26	3.34	42.5	37	3.45														
217	752.72	4485.73	98	6	191	19	18.39	3.66	*	*	26.9														
218	752.64	4486.59	350	4	255	49	7.14	2.85	53.3	25.4	14.8														
219	761.61	4482.39	26	18	138	52	15.86	2.88	15.5	26.1	2.97														
220	761.73	4483.17	201	16	305	42	20.58	2.58	8.4	20.8	12.0														
221	763.16	4483.21	219	7	125	32	14.26	2.98	15.8	7.3	28.5														
222	762.27	4481.43	98	1	287	89	17.84	1.52	34.5	22	5.05														
223	762.58	4480.39	213	23	98	43	20.48	1.34	*	*	14.6														
224	761.74	4479.50	184	24	316	53	17.65	1.75	27.5	24.9	16.2														
225	764.02	4482.49	27	31	*	*	19.77	1.47	40.4	65.7	5.55														
226	761.65	4477.97	297	39	47	26	18.73	1.70	64.5	22.2	5.74														
227	759.60	4481.35	35	12	132	31	15.24	3.30	23.5	8.7	9.76														
228	760.71	4481.11	30	8	130	50	18.05	2.45	33.7	29.7	5.37														
229	758.51	4482.51	*	*	94	27	15.11	1.84	30.7	*	5.59														
230	759.06	4478.78	182	18	83	28	15.17	1.95	11.7	24.7	5.91														
231	765.46	4480.18	181	32	56	45	11.67	1.23	46.5	22	9.76														
232	766.90	4481.01	240	43	95	54	17.63	1.22	47.1	41.2	8.48														
233	755.02	4483.56	184	41	301	30	13.63	1.54	24	25.8	6.3														
234	754.35	4482.48	331	20	87	52	16.10	2.78	11.1	14.8	9.1														
235	756.50	4484.28	5	7	264	60	14.49	2.30	18.8	23.2	20.2														
236	754.63	4485.05	186	4	26	79	13.66	2.01	42.5	40.4	12.9														
237	755.33	4479.35	337	49	236	11	12.29	2.75	37.9	18.7	11.7														
238	756.18	4480.59	22	15	123	34	10.44	2.04	10.9	28.8	34.4														
239	756.75	4482.26	205	1	296	52	15.50	3.61	12	10.9	2.51														
240	758.90	4480.36	23	1	293	23	12.08	2.63	40.1	14.3	5.32														
241	756.00	4477.81	195	33	79	35	13.77	2.67	32.5	20.7	15.9														

References

- Aller, J., Bastida, F., 1996. Geology of the Ollo de Sapo antiform unit to the south of the Cabo Ortegal complex (NW Spain). *Revista de la Sociedad Geológica de España* 9, 183–195.
- Amice, M., 1990. Le complexe granitique de Cabeza de Araya (Estrémadure, Espagne). Zonation, structures magmatiques et magnétiques, géométrie. Discussion du mode de mise en place. Ph.D. thesis, University Paul Sabatier, Toulouse.
- Anderson, E.M., 1951. The dynamics of faulting and dyke formation. Oliver & Boyd, Edinburgh 206 pp.
- Aranguren, A., Tubía, J.M., 1992. Structural evidence for the relationship between thrusts, extensional faults and granite intrusions in the Variscan belt of Galicia (Spain). *Journal of Structural Geology* 14, 1229–1237.
- Aranguren, A., 1993. Estructura y cinemática del emplazamiento de los granitoides del Domo de Lugo y del Antiforme del Ollo de Sapo. Ph.D. thesis, University of País Vasco.
- Archanjo, C.J., Bouchez, J.L., Corsini, M., Vauchez, A., 1994. The Pombal granite pluton: magnetic fabric, emplacement and relationships with the Brasiliano strike-slip setting of NE Brazil (Paraíba State). *Journal of Structural Geology* 16, 323–335.
- Bateman, R., 1985. Aureole deformation by flattening around a diapir during in situ ballooning: the Cannibal Creek granite. *Journal of Geology* 93, 293–310.
- Bea, F., Moreno-Ventas, I., 1985. Estudio petrológico de los granitoides del área centro-norte de la Sierra de Gredos (Batolito de Ávila; Sistema Central Español). *Studia Geologica Salmanticensia* 20, 137–174.
- Bea, F., Pereira, M.D., 1990. Estudio petrológico del Complejo Anatóctico de la Peña Negra (Batolito de Ávila). *Revista de la Sociedad Geológica de España* 3, 87–104.
- Bea, F., Sánchez González de Herrero, J.G., Serrano Pinto, M., 1987. Una compilación geoquímica (elementos mayores) de los granitoides del Macizo Hespérico. In: Bea, F., Carnicero, A., Gonzalo, J.C., López Plaza, M., Rodríguez Alonso, M.D. (Eds.), *Geología de los granitoides y rocas asociadas del Macizo Hespérico*. Rueda, Madrid, pp. 87–193.
- Bell, T.H., 1986. Foliation development and refraction in metamorphic rocks: reactivation of early foliations and decrenulation due to shifting patterns of deformation partitioning. *Journal of Metamorphic Geology* 4, 421–444.
- Benn, K., Genkin, M., Van Staal, C.R., Lin, S., 1993. Structure and anisotropy of magnetic susceptibility of the Rose Blanche granites, southwestern Newfoundland: kinematics and relative timing of emplacement. In: *Current Research, Part D*, Geology Survey Canada, Paper 93-1D, 73–82.
- Benn, K., 1994. Overprinting of magnetic fabrics in granites by small strains: numerical modelling. *Tectonophysics* 233, 153–162.
- Blumenfeld, Ph., Mainprice, D., Bouchez, J.L., 1986. C-slip in quartz from subsolidus deformed granite. *Tectonophysics* 127, 97–115.
- Borradaile, G.J., 1988. Magnetic susceptibility, petrofabrics and strain. *Tectonophysics* 156, 1–20.
- Bouchez, J.L., Gleizes, G., 1995. Two-stage deformation of the Mont-Louis–Andorra granite pluton (Variscan Pyrenees) inferred from magnetic susceptibility anisotropy. *Journal of the Geological Society of London* 152, 669–679.
- Bouchez, J.L., Bernier, S., Rochette, P., Guineberteau, B., 1987. Log des susceptibilités magnétiques et anisotropies de susceptibilité dans le granite de Beauvoir: conséquences pour sa mise en place. *Géologie de la France* 2–3, 223–232.
- Bouchez, J.L., Gleizes, G., Djouadi, T., Rochette, P., 1990. Microstructure and magnetic susceptibility applied to emplacement kinematics of granites: the example of the Foix pluton (French Pyrenees). *Tectonophysics* 184, 157–171.
- Bouchez, J.L., Delas, C., Gleizes, G., Nédélec, A., Cuney, M., 1992. Submagmatic microfractures in granites. *Geology* 20, 35–38.
- Bouchez, J.L., 1997. Granite is never isotropic: an introduction to AMS studies of granitic rocks. In: Bouchez, J.L., Hutton, D.H.W., Stephens, W.E. (Eds.), *Granite: From Segregation of Melt to Emplacement Fabrics*. Kluwer Academic Publishers, Dordrecht, The Netherlands, pp. 95–112.
- Bouillin, J.P., Bouchez, J.L., Lespinasse, P., Pécher, A., 1993. Granite emplacement in an extensional setting: an AMS study of the magmatic structures of Monte Capanne (Elba Italy). *Earth and Planetary Sciences Letters* 118, 263–279.
- Bowen, N.L., 1948. The granite problem and the method of multiple prejudices. In: Gilluly, J., (Ed.), *Origin of granites*. Geological Society of America Memoires 28, pp. 79–90.
- Brisbin, W.C., Green, A.G., 1980. Gravity model of the Aulneau batholith, northwestern Ontario. *Canadian Journal of Earth Sciences* 17, 968–977.
- Brun, J.P., Pons, J., 1981. Strain patterns of pluton emplacement in a crust undergoing non-coaxial deformation, Sierra Morena, Southern Spain. *Journal of Structural Geology* 3, 219–229.
- Brun, J.P., Gapais, D., Cogné, J.P., Ledru, P., Vigneresse, J.L., 1990. The Flamanville Granite (Northwest France): an unequivocal example of a syntectonically expanding pluton. *Geological Journal* 25, 271–286.
- Castro, A., 1987. On granitoid emplacement and related structures. A review. *Geologische Rundschau* 76, 101–124.
- Clemens, J.D., Mawer, C.K., 1992. Granitic magma transport by fracture propagation. *Tectonophysics* 204, 339–360.
- Collins, W.J., Sawyer, E.W., 1996. Pervasive granitoid magma transfer through the lower-middle crust during non-coaxial compressional deformation. *Journal of Metamorphic Geology* 14, 565–579.
- Cook, J., Gordon, J.E., 1964. A mechanism for the control of crack propagation in all-brittle systems. *Proceedings of the Royal Society of London* 282, 508–520.
- Cordell, L., Henderson, R.G., 1968. Iterative three dimensional solution of gravity anomaly used a digital computer. *Geophysics* 33, 596–601.
- Cruden, A.R., 1998. On the emplacement of tabular granites. *Journal of the Geological Society of London* 155, 853–862.
- D’Lemos, R.S., Brown, M., Strachan, R.A., 1992. Granite magma generation, ascent and emplacement in a transpressional orogen. *Journal of the Geological Society of London* 149, 487–490.
- Daly, S.F., Raefsky, A., 1985. On the penetration of a hot diapir through a strongly temperature-dependent viscosity medium. *Geophysical Journal of the Royal Astronomical Society* 83, 657–682.
- Davis, B.K., 1993. Mechanism of emplacement of the Cannibal Creek Granite with special reference to timing and deformation history of the aureole. *Tectonophysics* 224, 337–362.
- Dehls, J.F., Cruden, A.R., Vigneresse, J.L., 1997. Fracture control of pluton emplacement in the northern Slave Province. *Geological Association of Canada Program with Abstracts* 22, A36.
- Dewey, J.F., 1988. Extensional collapse of orogens. *Tectonics* 7, 1123–1139.
- Díez Balda, M.A., Vegas, R., González Lodeiro, F., 1990. Structure of the Central Iberian Zone. In: Dallmeyer, R.D., Martínez García, E. (Eds.), *Pre-Mesozoic Geology of Iberia*. Springer, Berlin, pp. 172–188.
- Díez Balda, M.A., Martínez Catalán, J.R., Ayarza Arribas, P., 1994. Syn-collisional extensional collapse parallel to the orogenic trend in a domain of steep tectonics: the Salamanca Detachment Zone (Central Iberian Zone, Spain). *Journal of Structural Geology* 17, 163–182.
- Diot, H., 1989. Mise en place des granitoides hercyniens de la Meseta Marocaine. Etude structurale des massifs de Sebte de Brikiine (Rehamna), de Zaër et d’Oulmès (Massif Central), et d’Aouli Bou-Mia (Haute Moulouya). Implications géodynamiques. Ph.D. thesis, University Paul Sabatier, Toulouse.
- England, R.W., 1990. The identification of granitic diapirs. *Journal of the Geological Society of London* 147, 931–933.
- Ernst, R.E., Pearce, G.W., 1989. Averaging of anisotropy of mag-

- netic susceptibility data. In: Agterberg, F.P. and Bonham-Carter G.F.G. (Eds.), *Statistical Applications in the Environment*. Paper of the Geology Survey of Canada 89-9, pp. 297–305.
- Evans, D.J., Rowley, W.J., Chadwick, R.A., Kimbell, G.S., Millward, D., 1994. Seismic reflection data and internal structure of the Lake District batholith, Cumbria, northern England. *Proceedings of the Yorkshire Geological Society* 50, 11–24.
- Evans, N.G., Gleizes, G., Leblanc, D., Bouchez, J.L., 1997. Hercynian tectonics in the Pyrenees: a new view based on structural observations around the Bassiès granite pluton. *Journal of Structural Geology* 19, 195–208.
- Ferré, E., Gleizes, G., Bouchez, J.L., Nnabo, P.N., 1995. Internal fabric and strike-slip emplacement of the Pan-African granite of Solli Hills, northern Nigeria. *Tectonics* 14, 1205–1219.
- Fisher, R.A., 1953. Dispersion on a sphere. *Proceedings of the Royal Society of London* 217, 295–305.
- Flinn, D., 1962. On folding during three dimensional progressive deformation. *Quarterly Journal of the Geological Society of London* 118, 385–428.
- Franco, M.P., García de Figuerola, L.C., 1986. Las rocas básicas y ultrabásicas en el extremo occidental de la Sierra de Ávila (Provincias de Ávila y Salamanca). *Studia Geologica Salamanticensis* 23, 193–219.
- Fúster, J.M., Villaseca, C., 1987. El complejo plutónico hercínico-tardihercínico del Sistema Central Español. In: Bea, F., Carnicero, A., Gonzalo, J.C., López Plaza, M., Rodríguez Alonso, M.D. (Eds.), *Geología de los granitoides y rocas asociadas del Macizo Hespérico*. Rueda, Madrid, pp. 27–35.
- Galibert, F., 1984. *Géochimie et géochronologie du Complexe granitique de l'antiforme de Morille (Salamanque, Espagne)*. Rapport de Stage de D.E.A., Lab. de Géochimie Isotopique, University of Montpellier, 53 p.
- Gapais, D., Barbarin, B., 1986. Quartz fabric transition in a cooling syntectonic granite (Hermitage massif, France). *Tectonophysics* 125, 357–370.
- Gleizes, G., 1992. *Structure des granites hercyniens des Pyrénées. De Mont-Louis-Andorre à La Maladeta*. Ph.D. thesis, University Paul Sabatier, Toulouse.
- Graham, J.W., 1954. Magnetic anisotropy, an unexploited petrofabric element. *Geological Society of America Bulletin* 65, 1257–1258.
- Guglielmo Jr, G., 1993a. Magmatic strains foliation triple points of the Merrimac plutons, northern Sierra Nevada, California: implications for pluton emplacement and timing of subduction. *Journal of Structural Geology* 15, 177–189.
- Guglielmo Jr, G., 1993b. Interference between pluton expansion and non-coaxial tectonic deformation: three-dimensional computer model and field implications. *Journal of Structural Geology* 15, 593–608.
- Guillet, Ph., Bouchez, J.L., Wagner, J.J., 1983. Anisotropy of magnetic susceptibility and magmatic structures in the Guérande granite massif (France). *Tectonics* 2, 419–429.
- Guineberteau, B., Bouchez, J.L., Vigeneresse, J.L., 1987. The Mortagne granite pluton (France) emplaced by pull-apart along a shear zone: structural and gravimetric arguments and regional implications. *Geological Society of America Bulletin* 99, 763–770.
- Hamilton, W., Myers, W.B., 1967. *The nature of batholiths*. Geological Survey Professional Papers.
- Hibbard, M.J., 1987. Deformation of incompletely crystallised magma systems, granitic gneisses and their tectonic implications. *Journal of Geology* 95, 543–561.
- Hobbs, B.E., 1981. The influence of metamorphic environment upon the deformation of minerals. *Tectonophysics* 78, 335–383.
- Hollister, L.S., Crawford, M.L., 1986. Melt-enhanced deformation: a major tectonic process. *Geology* 14, 558–561.
- Hrouda, F., 1982. Magnetic anisotropy of rocks and its application in geology and geophysics. *Geophysical Survey* 5, 37–82.
- Hrouda, F., 1986. The effect of quartz on the magnetic anisotropy of quartzite. *Studia Geophysica Geodynamica* 30, 39–45.
- Hutton, D.H.W., 1997. Syntectonic granites and the principle of effective stress: a general solution to the space problem? In: Bouchez, J.L., Hutton, D.H.W., Stephens, W.E. (Eds.), *Granite: From Segregation of Melt to Emplacement Fabrics*. Kluwer Academic Publishers, Dordrecht, The Netherlands, pp. 189–197.
- Hutton, D.H.W., 1988. Granite emplacement mechanisms and tectonic controls, inferences from deformation studies. *Transactions of the Royal Society of Edinburgh, Earth Sciences* 79, 245–255.
- Hutton, D.H.W., 1992. Granite sheeted complexes: evidence for the dyking ascent mechanism. *Transactions of the Royal Society of Edinburgh, Earth Sciences* 83, 377–382.
- Ingram, G.M., Hutton, D.H.W., 1994. The Great Tonalite Sill: emplacement into a contractional shear zone and implications for Late Cretaceous to early Eocene tectonics in southeastern Alaska and British Columbia. *Geological Society of America Bulletin* 106, 715–728.
- Jelinek, V., 1981. Characterization of the magnetic fabric of rocks. *Tectonophysics* 79, 63–67.
- Julivert, M., Fonboté, J.M., Ribeiro, A., Nabais Conde, L.E., 1972. Mapa tectónico de la Península Ibérica y Baleares, E: 1:1.000.000. Instituto Geológico y Minero de España.
- Karlstrom, K.E., Miller, C.F., Kingsbury, J.A., Wooden, J.L., 1993. Pluton emplacement along an active ductile thrust zone, Piute Mountains, southeastern California: interaction between deformational and solidification processes. *Geological Society of America Bulletin* 105, 213–230.
- King, R.F., 1966. The magnetic fabric of some Irish granites. *Journal of Geology* 5, 43–66.
- Lagarde, J.L., Ait-Omar, S., Roddaz, B., 1990a. Structural characteristics of granitic plutons emplaced during weak regional deformation: examples from late Carboniferous plutons, Morocco. *Journal of Structural Geology* 12, 805–821.
- Lagarde, J.L., Brun, J.P., Gapais, D., 1990b. Formation des plutons granitiques par injection et expansion latérale dans leur site de mise en place: une alternative au diapirisme en domaine épizonal. *Comptes Rendue de l'Academie Sciences de Paris, Série II* 310, 1109–1114.
- Leblanc, D., Gleizes, G., Lespinasse, P., Olivier, Ph., Bouchez, J.L., 1994. The Maladeta granite polydiapir, Spanish Pyrenees: a detailed magneto-structural study. *Journal of Structural Geology* 16, 223–235.
- Lister, G.S., Dornsiepen, U.F., 1982. Fabric transitions in the Saxony granulite terrain. *Journal of Structural Geology* 4, 81–92.
- López Plaza, M., Martínez Catalán, J.R., 1987. Síntesis estructural de los granitoides del Macizo Hespérico. In: Bea, F., Carnicero, A., Gonzalo, J.C., López Plaza, M., Rodríguez Alonso, M.D. (Eds.), *Geología de los granitoides y rocas asociadas del Macizo Hespérico*. Rueda, Madrid, pp. 195–210.
- Macaya, J., González Lodeiro, F., Martínez Catalán, J.R., Álvarez, F., 1991. Continuous deformation, ductile thrusting and back-folding in the basement of the Hercynian orogen and their relationships with structures in the metasedimentary cover in the Spanish Central System. *Tectonophysics* 191, 291–309.
- Mahon, K.I., Harrison, T.M., Drew, D.A., 1988. Ascent of a granitoid diapir in a temperature varying medium. *Journal of Geophysical Research* 93, 1174–1188.
- Mainprice, D., Nicolas, A., 1989. Development of shape and lattice preferred orientations: application to the seismic anisotropy of the lower crust. *Journal of Structural Geology* 11, 175–189.
- Mainprice, D., Bouchez, J.L., Blumenfeld, Ph., Tubía, J.M., 1986. Dominant *c* slip in naturally deformed quartz: implications for dramatic plastic softening at high temperature. *Geology* 14, 819–822.
- Marre, J., 1982. *Méthodes d'analyse structurale des granitoides*. BRGM, n° 3, 126 p.
- Marsh, B.D., 1982. On the mechanics of igneous diapirism, stoping and zone melting. *American Journal of Science* 282, 808–885.
- McCaffrey, K.J.W., Petford, N., 1997. Are granitic intrusions scale invariant? *Journal of the Geological Society of London* 154, 1–4.

- McCaffrey, K.J.W., 1992. Igneous emplacement in a transpressive shear zone: Ox Mountains Igneous Complex. *Journal of the Geological Society of London* 149, 221–235.
- Meneilly, A.W., 1982. Regional structure and syntectonic granite intrusion in the Dalradian of the Gweebarra Bay area, Donegal. *Journal of the Geological Society of London* 139, 633–646.
- Meneilly, A.W., 1983. Development of early composite cleavage in pelites from West Donegal. *Journal of Structural Geology* 5, 83–97.
- Morand, V.J., 1992. Pluton emplacement in a strike-slip fault zone: the Doctors Flat Pluton, Victoria, Australia. *Journal of Structural Geology* 14, 205–213.
- Moreno-Ventas, I., Rogers, G., Castro, A., 1995. The role of hybridization in the genesis of Hercynian granitoids in the Gredos Massif, Spain: inferences from Sm–Nd isotopes. *Contributions to Mineralogy and Petrology* 120, 137–149.
- Myers, J.S., 1975. Cauldron subsidence and fluidization: mechanism of intrusion of the coastal batholith of Peru into its own volcanic ejecta. *Geological Society of America Bulletin* 86, 1209–1220.
- Nagata, T., 1961. *Rock Magnetism*. Maruzen, Tokyo.
- Parsons, T., Sleep, N.H., Thompson, A., 1992. Host rock rheology controls on the emplacement of tabular intrusions: implications for underplating of extending crust. *Tectonics* 11, 1348–1356.
- Paterson, S.R., Vernon, R.H., Tobisch, O.T., 1989. A review of criteria for the identification of magmatic and tectonic foliations in granitoids. *Journal of Structural Geology* 11, 349–363.
- Paterson, S.R., Fowler Jr, T.K., 1993. Re-examining pluton emplacement processes. *Journal of Structural Geology* 15, 191–206.
- Petford, N., 1996. Dykes or diapirs. *Transactions of the Royal Society of Edinburgh, Earth Sciences* 87, 105–114.
- Pitcher, W.S., Berger, A.R., 1972. *The Geology of Donegal: A Study of Granite Emplacement and Unroofing*. Wiley-Interscience, New York.
- Pryer, L.L., 1993. Microstructures in feldspars from a major crustal thrust zone: the Grenville Front, Ontario, Canada. *Journal of Structural Geology* 15, 21–36.
- Ramberg, H., 1981. *Gravity, Deformation and the Earth's Crust*. Academic Press, London.
- Recio, C., 1990. The late Hercynian granitoids of the western area of the SCE: a stable (O, H, S) isotopic study. Ph.D. thesis, University of Salamanca.
- Riller, U., Cruden, A.R., Schwerdtner, W.M., 1996. Magnetic fabric and microstructural evidence for a tectono-thermal overprint of the early Proterozoic Murray pluton, central Ontario, Canada. *Journal of Structural Geology* 18, 1005–1016.
- Rochette, P., 1987. Magnetic susceptibility of the rock matrix related to magnetic fabrics studies. *Journal of Structural Geology* 9, 1015–1020.
- Román Berdiel, M.T., Pueyo Morer, E.L., Casas Sainz, A.M., 1995. Granite emplacement during contemporary shortening and normal faulting: structural and magnetic study of the Veiga Massif (NW Spain). *Journal of Structural Geology* 17, 1689–1706.
- Román Berdiel, M.T., 1994. Mécanismes d'intrusion des granites supracrustaux: modèles analogiques et exemples naturels. Ph.D. thesis, University of Rennes I.
- Rousset, R., Daly, L., 1969. Sur la cohérence de la foliation magnétique du granite porphyroïde d'Egletons (Corrèze). *Comptes Rendue de l'Académie des Sciences de Paris, Série D* 268, 1912–1915.
- Sanderson, D.J., Meneilly, A.W., 1981. Analysis of three-dimensional strain modified uniform distributions: andalusite fabrics from a granite aureole. *Journal of Structural Geology* 3, 109–116.
- Schmidt, C.J., Smedes, H.W., O'Neill, J.M., 1990. Syncompressional emplacement of the Boulder and Tobacco Root Batholiths (Montana U.S.A.) by pull apart along old fault zones. *Geological Journal* 25, 305–318.
- Schwerdtner, W.M., 1995. Local displacement of diapir contacts and its importance to pluton emplacement study. *Journal of Structural Geology* 17, 907–910.
- Shaw, H.R., 1980. Fracture mechanisms of magma transport from the mantle to the surface. In: Hargraves, R.B. (Ed.), *Physics of magmatic processes*. Princeton University Press, pp. 201–264.
- Simpson, C., Wintsch, R.P., 1989. Evidence for deformation-induced K-feldspar replacement by myrmekite. *Journal of Metamorphic Geology* 7, 261–275.
- Simpson, C., 1985. Deformation of granitic rocks across the brittle–ductile transition. *Journal of Structural Geology* 7, 503–511.
- Smart, T.B., 1962. The aureole of the Barnesmore granite, County Donegal. *Irish National Journal* 14, 55–59.
- Speer, J.A., McSween Jr, H.Y., Gates, A.E., 1994. Generation, segregation, ascent and emplacement of Alleghanian plutons in the southern Appalachians. *Journal of Geology* 102, 249–267.
- Takeshita, T., Wenk, H.R., 1988. Plastic anisotropy and geometrical hardening in quartzites. *Tectonophysics* 149, 345–361.
- Tarling, D.H., Hrouda, F., 1993. *The Magnetic Anisotropy of Rocks*. Chapman & Hall, London.
- Tobisch, O.T., Paterson, S.R., 1990. The Yarra granite: an intradeformational pluton associated with ductile thrusting, Lachlan Fold belt, southeastern Australia. *Geological Society of America Bulletin* 102, 693–703.
- Tribe, I.R., D'Lemos, R.S., 1996. Significance of a hiatus in down-temperature fabric development within syn-tectonic quartz diorite complexes, Channel Islands, UK. *Journal of the Geological Society of London* 153, 127–138.
- Tribe, J.R., Strachan, R.A., D'Lemos, R.S., 1996. Neoproterozoic shear zone tectonics within the Icartian basement of Guernsey and Sark, Channel Islands. *Geological Magazine* 133, 177–192.
- Ugidos, J.M., Recio, C., 1993. Origin of cordierite-bearing granites by assimilation in the Central Iberian Massif (CIM), Spain. *Chemical Geology* 103, 27–43.
- Ugidos, J.M., Rodríguez Alonso, M.D., Albert Colomert, V., Martín Herrero, D., 1990. Mapa Geológico de España E. 1:50.000, Hoja n° 552 (12-22) (Miranda del Castañar). Instituto Tecnológico y Geominero de España, Madrid 77 pp.
- Ugidos, J.M., 1973. Estudio petrológico del área Béjar–Plasencia (Salamanca–Cáceres). Ph.D. thesis, University of Salamanca.
- Vauchez, A., 1980. Ribbon texture and deformation mechanisms in quartz in a mylonitized granite of Great Kabylia (Algeria). *Tectonophysics* 67, 1–2.
- Vidal, G., Palacios, T., Gamez, J.A., Díez Balda, M.A., Grant, S.W., 1994. Neoproterozoic–Cambrian Iberian geology and paleontology. *Geological Magazine* 131, 729–765.
- Vignerresse, J.L., 1978. Damped and constrained least squares method with application to gravity interpretation. *Journal of Geophysics* 45, 17–28.
- Vignerresse, J.L., 1983. Enracinement des granites armoricains estimé d'après la gravimétrie. *Bulletin de la Societe Geologique et Mineralogique Bretagne* 15C, 1–15.
- Vignerresse, J.L., 1990. Use and misuse of geophysical data to determine the shape at depth of granitic intrusions. *Geological Journal* 25, 249–260.
- Vignerresse, J.L., 1995. Control of granite emplacement by regional deformation. *Tectonophysics* 249, 173–186.
- Yenes, M., Gutiérrez Alonso, G., Álvarez, F., Díez Balda, M.A., Vignerresse, J.L., 1995. Aproximación a un modelo gravimétrico en tres dimensiones (3D) de los granitoides del área de La Alberca–Béjar (Zona Centro–Ibérica). *Revista de la Sociedad Geológica de España* 8, 51–59.
- Yenes, M., Gutiérrez Alonso, G., Álvarez, F., 1996. Dataciones K–Ar de los granitoides del área La Alberca–Béjar (Sistema Central Español). *Geogaceta* 20, 224–227.
- Yenes, M., 1996. Estructura, geometría y cinemática del emplazamiento de los granitoides del área de La Alberca–Béjar (Sistema Central Español, Zona Centro–Ibérica). Ph.D. thesis, University of Salamanca.